




Human Umbilical Cord Mesenchymal Stem Cells for the Treatment of Systemic Lupus Erythematosus via Glucose Metabolism of CD4⁺T Cells

Meng Ding¹ · Lu Jin¹ · Shaoxin Cui¹ · Lin Yang¹ · Jingjing He¹ · Xiaoping Wang¹ · Fei Chang¹ · Qun Wang¹ · Xue Liu¹ · Hongtao Jin¹ · Shuran Song^{2,3} · Min Shi^{2,3} · Jingjing Yu^{1,5} · Jun Ma^{4,5} · Aijing Liu^{1,3,5} 

Accepted: 31 January 2025 / Published online: 20 February 2025
© The Author(s) 2025

Abstract

Background T cells play a crucial role in the pathogenesis of systemic lupus erythematosus (SLE), with their functions regulated by various metabolic pathways. This study explores SLE pathogenesis and the therapeutic effects of human umbilical cord-derived mesenchymal stem cells (hUC-MSCs) via metabolic reprogramming.

Methods Clinical data and peripheral blood samples were collected from 15 SLE patients and matched healthy controls. CD4⁺ T cells were isolated and activated in vitro with anti-CD3/CD28. Following 72 h of co-culture with hUC-MSCs, CD4⁺ T cell viability was assessed using the CCK-8 assay. The oxygen consumption rate (OCR) and glycolytic proton efflux rate (glycoPER) were measured with a Seahorse analyzer. Cytokine levels were detected by multiplex assay, and transcriptome sequencing was performed. Western blotting analyzed glucose metabolism-related enzymes and signaling pathways in lupus model mice.

Results Compared to healthy controls, activated CD4⁺ T cells from SLE patients exhibited significantly increased OCR and glycoPER levels ($P < 0.05$). Following 72 h of co-culture with hUC-MSCs, OCR, glycoPER, cell viability, and pro-inflammatory factors in SLE-CD4⁺ T cells decreased markedly ($P < 0.01$). Upregulation of 434 genes and downregulation of 172 genes was observed, particularly in the JAK-STAT and PI3K-Akt pathways. hUC-MSCs inhibited the expression of glucose metabolism-related enzymes and the JAK-STAT and PI3K-Akt signaling pathways in lupus model mice.

Conclusion hUC-MSCs inhibited the proliferation and function of aberrant CD4⁺ T cells in SLE patients by modulating glycometabolism and the JAK-STAT and PI3K-Akt signaling pathways, providing new insights into the therapeutic mechanisms of MSCs based on metabolic reprogramming.

Keywords Systemic lupus erythematosus · CD4⁺ T lymphocytes · Metabolic reprogramming · Glycolysis · Mesenchymal stem cells · mRNA

Meng Ding, Lu Jin, Shaoxin Cui and Lin Yang contributed equally.

✉ Aijing Liu
Laj111@126.com

Jun Ma
13933113125@163.com

¹ Department of Rheumatology and Immunology, The Second Hospital of Hebei Medical University, Shijiazhuang 050000, Hebei Province, China

² Department of Clinical Laboratory, The Second Hospital of Hebei Medical University, Shijiazhuang 050000, Hebei Province, China

³ Hebei Key Laboratory of Laboratory Medicine, The Second Hospital of Hebei Medical University, Shijiazhuang 050000, Hebei Province, China

⁴ Department of Anatomy, Hebei Medical University, Shijiazhuang 050000, Hebei Province, China

⁵ Hebei Research Center for Stem Cell Medical Translational Engineering, Shijiazhuang 050000, Hebei Province, China

Background

Systemic lupus erythematosus (SLE) is a highly heterogeneous autoimmune disease characterized by the activation of immune effector cells resulting from an imbalance in immune tolerance, which leads to the production of numerous cytokines and autoantibodies [1]. The generation of these autoantibodies depends on T cells, particularly autoreactive CD4⁺ T cells, which provide co-stimulatory signals and cytokines to autoreactive B cells [2]. These signals stimulate B cells to secrete autoantibodies and form immune complexes that are deposited in target organs, ultimately causing inflammation and tissue damage [3].

The proliferative and/or functional imbalance of T cells is vital for the immunopathogenesis of SLE, with several studies indicating that these anomalies are associated with aberrant metabolic levels [4, 5]. In 2002, Frauwirth confirmed that CD28 co-stimulatory signals promote glucose uptake by CD4⁺ T cells via the phosphoinositide 3-kinase (PI3K) pathway [6], which first demonstrated the correlation between metabolism and immune cell activation. SLE-CD4⁺ T cells exhibit overactivation and increased glycolytic activity, resembling the Warburg effect observed in tumors [7]. In addition, CD4⁺ T cells also show mitochondrial dysfunction, membrane hyperpolarization, and elevated levels of oxidative metabolism [8]. Targeting T cell glycometabolism has been shown to facilitate disease remission in SLE [9].

The current conventional treatments used for SLE include glucocorticoids, cyclophosphamide, mycophenolate mofetil, azathioprine, and methotrexate. Although efficacious in SLE patients, the disease cannot be controlled satisfactorily in some patients due to the serious side effects of the drugs or poor treatment response. Some severe patients (involving the kidneys, heart, lungs, and nervous system) show continual disease advancement, and the 10-year mortality rate is approximately 10% [10]. In recent years, several new biologics, including belimumab, rituximab, and abatacept, have emerged, yet they possess certain limitations, such as increased risk of infection and high costs [11]. Moreover, some patients remain non-responsive or experience recurrence despite these therapies [12]. Therefore, there is a pressing need to develop effective treatments with fewer side effects based on new immunomodulatory and immunosuppressive treatments. Recently, mesenchymal stem cells (MSCs) have garnered substantial attention as a novel treatment for autoimmune diseases due to their anti-inflammatory properties [13], immunomodulatory effects [14], and capacity for tissue repair. Studies indicate that MSCs inhibit the proliferation and cytokine secretion of CD3⁺ T cells [15], suppress the proliferation and autoantibody production of CD19⁺ B cells [16], prevent

the maturation of dendritic cells [17], and block the cytotoxic effects of natural killer cells [18]. MSCs demonstrate promising efficacy and safety in treating SLE by reducing inflammatory responses and inhibiting the activation of inflammatory pathways and cells [19]. However, the specific mechanism of MSCs in the treatment of SLE is yet to be elucidated.

In this study, we explored the effects of human umbilical cord-derived mesenchymal stem cells (hUC-MSCs) on the proliferation capacity, function and glucose metabolism of peripheral CD4⁺ T cells in patients with SLE. Also, we elucidated the pathogenesis of SLE and possible therapeutic mechanism of hUC-MSCs based on metabolic reprogramming.

Materials and Methods

Study Population

A total of 15 treatment-naïve SLE patients and 15 healthy age- and gender-matched controls were recruited from the Department of Rheumatology and Immunology of the Second Hospital of Hebei Medical University between August 2021 and February 2022. All the patients met the 2019 EULAR/ACR classification criteria [20]. Patients were excluded if they met any of the following criteria: ① aged < 18 years or > 70 years, ② diagnosed with infectious, metabolic, or other autoimmune diseases, ③ diagnosed with malignancy, ④ diagnosed with any other chronic diseases, ⑤ using metformin, ⑥ having graft-versus-host disease.

Clinical data, demographic characteristics, and laboratory findings were collected, including age, gender, body mass index (BMI), disease duration, systemic involvement (skin and mucosa, joints, hematological system, serositis, renal system, and neurological system), immune markers (e.g., autoantibodies, immunoglobulins, and complements), and the Systemic Lupus Erythematosus Disease Activity Index 2000 (SLEDAI-2 K). This study was approved by the Ethics Committee of the Second Hospital of Hebei Medical University (2021-R392), and all participants provided written informed consent.

Mice

Female MRL/lpr mice and female C57BL/6 mice were obtained from Beijing Spefo Biotech Co. (Beijing, China). The mice were housed under specific pathogen-free conditions in the animal facility at Hebei Medical University. All animal experiments were approved by the Animal Experimentation Committee of Hebei Medical University (2023-AE-164).

Isolation, Culture, and Activation of CD4⁺ T Cells

Peripheral venous blood was collected from all participants. Peripheral blood mononuclear cells were isolated by density gradient centrifugation. Peripheral blood CD4⁺ T cells were obtained by magnetic separation with Cell Separation Magnet (BD Biosciences, San Jose, CA, USA), followed by co-culture in the presence of 10 µg/mL CD3 and 5 µg/mL CD28 antibody (Leinco Technologies, St. Louis, Missouri, USA) for 72 h in vitro.

Detection of Glucose and Lactate in Cell Culture Supernatant

Cell culture supernatant was collected, and the levels of glucose and lactate were measured using the Glucose Assay Kit and Lactic Acid Assay Kit (Jiancheng, Nanjing, China), respectively. The procedures were performed according to the manufacturer's instructions.

Co-culture of CD4⁺ T Cells in SLE Patients with hUC-MSCs

SLE-CD4⁺ T cells were co-cultured with third-generation hUC-MSCs at ratio gradients of 5:1, 10:1 and 50:1 (T cells: MSCs). CD4⁺ T cells were inoculated at a density of 5×10^5 cells per well in the upper chamber of the transwell (0.4 µm pore size), while hUC-MSCs were inoculated at densities of 1×10^5 , 5×10^4 , and 1×10^4 cells per well in the lower chamber. The hUC-MSCs were obtained from Shandong Qilu Cell Therapy Engineering Technology Co. Ltd. (Qingdao, China) and met the criteria set by the International Society for Cellular Therapy to define MSCs [21]. To determine whether the hUC-MSCs met the established criteria, their morphology was observed under an inverted microscope (CKX41, OLYMPUS, Tokyo, Japan) during passaging. The hUC-MSCs were adherent cells exhibiting spindle-shaped characteristics similar to fibroblasts (Fig. 1a). The results of osteogenic, adipogenic, and chondrogenic differentiation were assessed using alizarin red S staining, oil red O staining, alcian blue staining and safranin O staining (Fig. 1b–e). Flow cytometry was employed to analyze the expression of surface markers: CD44⁺/CD90⁺/CD73⁺/CD105⁺ ≥ 95%; CD45⁺/CD34⁺/CD19⁺/CD11b⁺/HLA-DR⁺ ≤ 2% (Fig. 2).

Cell Proliferation Detection by Cell Counting Kit(CCK)–8 Assay

Cell viability was assessed using the CCK-8 assay (Sharebio, Shanghai, China) according to the manufacturer's instructions.

Energy Metabolism Assay

The Seahorse Bioscience XFe24 Extracellular Flux Analyzer (Agilent Technologies, California, USA) was used to measure the mitochondrial pressure by oxygen consumption rate (OCR) and glycolysis by the extracellular acidification rate (ECAR) of CD4⁺ T cells. The glycolytic proton efflux rate (glycoPER), a derivation of ECAR, could be calculated as a quantitative index of glycolytic rate. The Mito Stress Test (Mito Stress Test Kit, Agilent Technologies, California, USA) and Glycolytic Rate Assay (Glycolytic Rate Assay Kit, Agilent Technologies, California, USA) were conducted according to the manufacturer's instructions.

Cytokine Detection

A multiplex cytokine assay was conducted to measure the cytokines in the supernatant using flow microsphere assay technology and the Human Cytokine Screening Panel (BioPlex Pro™, Shanghai, China).

Transcriptome Sequencing

Transcriptome sequencing was performed on SLE-CD4⁺ T cells cultured alone or co-cultured with hUC-MSCs for 72 h. Total RNA was extracted from the samples using trizol reagent, and paired-end libraries were prepared with the ABclonal mRNA-seq Library Preparation Kit (ABclonal, Wuhan, China) and sequenced on the Illumina NovaSeq 6000 system following the provided instructions. Differentially expressed genes (DEGs) were identified using DESeq2 with cutoff values of $|\log_2FC| > 1$ and $P_{adj} < 0.05$, followed by analyses of functional enrichment, signaling pathways, and hub gene identification.

Real-time Quantitative Polymerase Chain Reaction(q-PCR)

Total RNA was extracted from CD4⁺ T cells before and after co-culture utilizing trizol solution (Servicebio, Wuhan, China), according to the manufacturer's instructions. q-PCR was conducted using cDNA synthesized with SweScript All-in-One RT SuperMix and Universal Blue SYBR Green qPCR Master Mix (both purchased from Servicebio, Wuhan, China), along with specific RNA primers. The relative expression of RNAs was determined and calculated using the $2^{-\Delta\Delta CT}$ method.

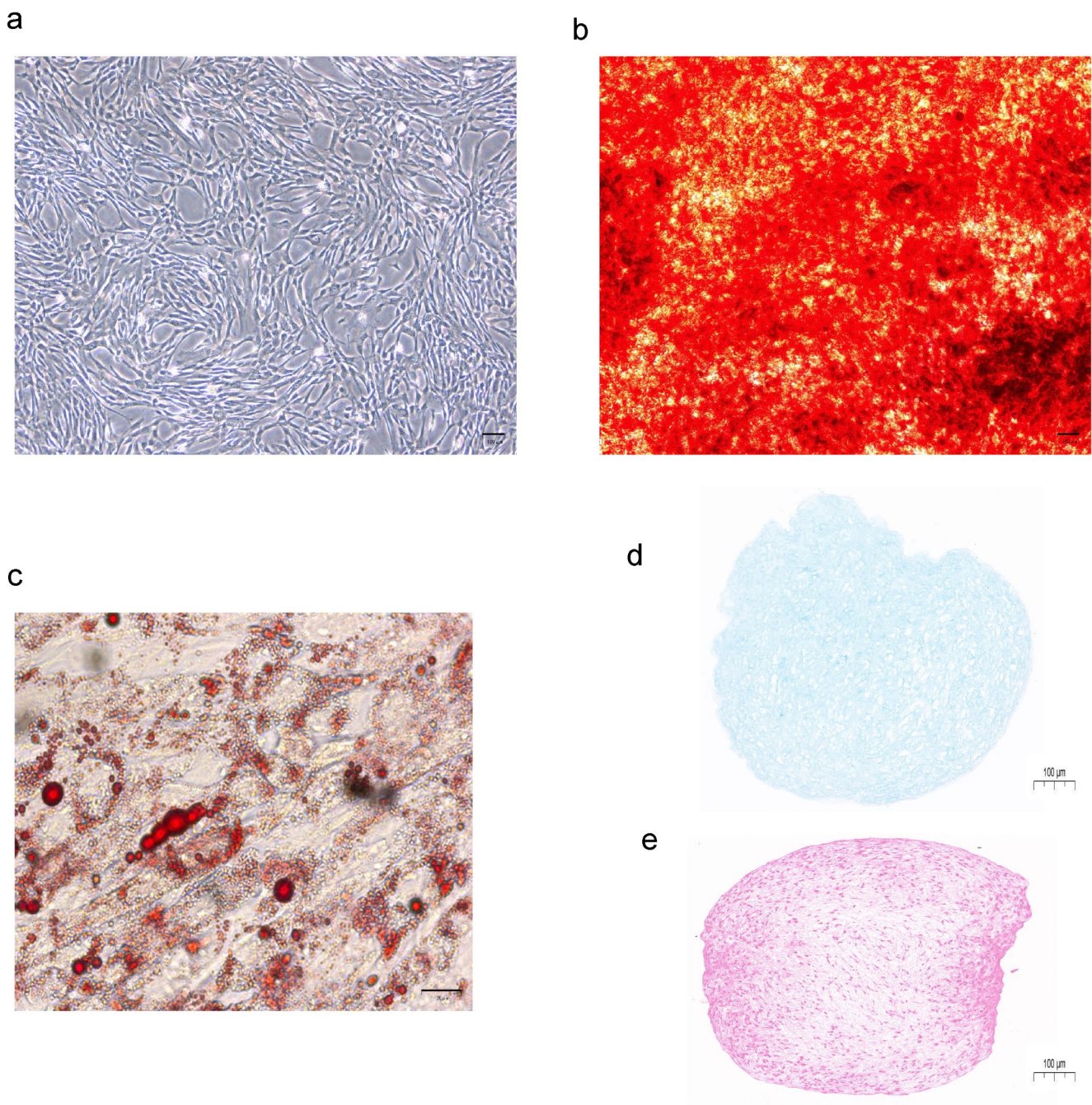


Fig. 1 Identification of morphology and differentiation potential of hUC-MSCs. **(a)** The morphology of cultured hUC-MSCs in the third generation was observed under inverted microscope. **(b)** Osteogenesis

via alizarin red S staining. **(c)** Adipogenesis via oil red O staining. **(d)** **(e)** Chondrogenesis via alcian blue staining and safranin O staining

Mice Grouping and Treatment

Six 8-week-old female MRL/lpr mice were randomly assigned to the SLE+MSCs group ($n=3$) or the SLE+phosphate buffered saline (PBS) group ($n=3$). Additionally, three age-matched female C57BL/6 mice were included as a control

group. At 16 weeks of age, mice in the SLE+MSCs group received a tail vein injection of 200 μ l of PBS containing 8×10^5 hUC-MSCs, while the SLE+PBS and control groups received 200 μ l of PBS alone via tail vein injection. A second injection of the same dose of hUC-MSCs or PBS was administered at 18 weeks. Mice were euthanized at 20 weeks of age.

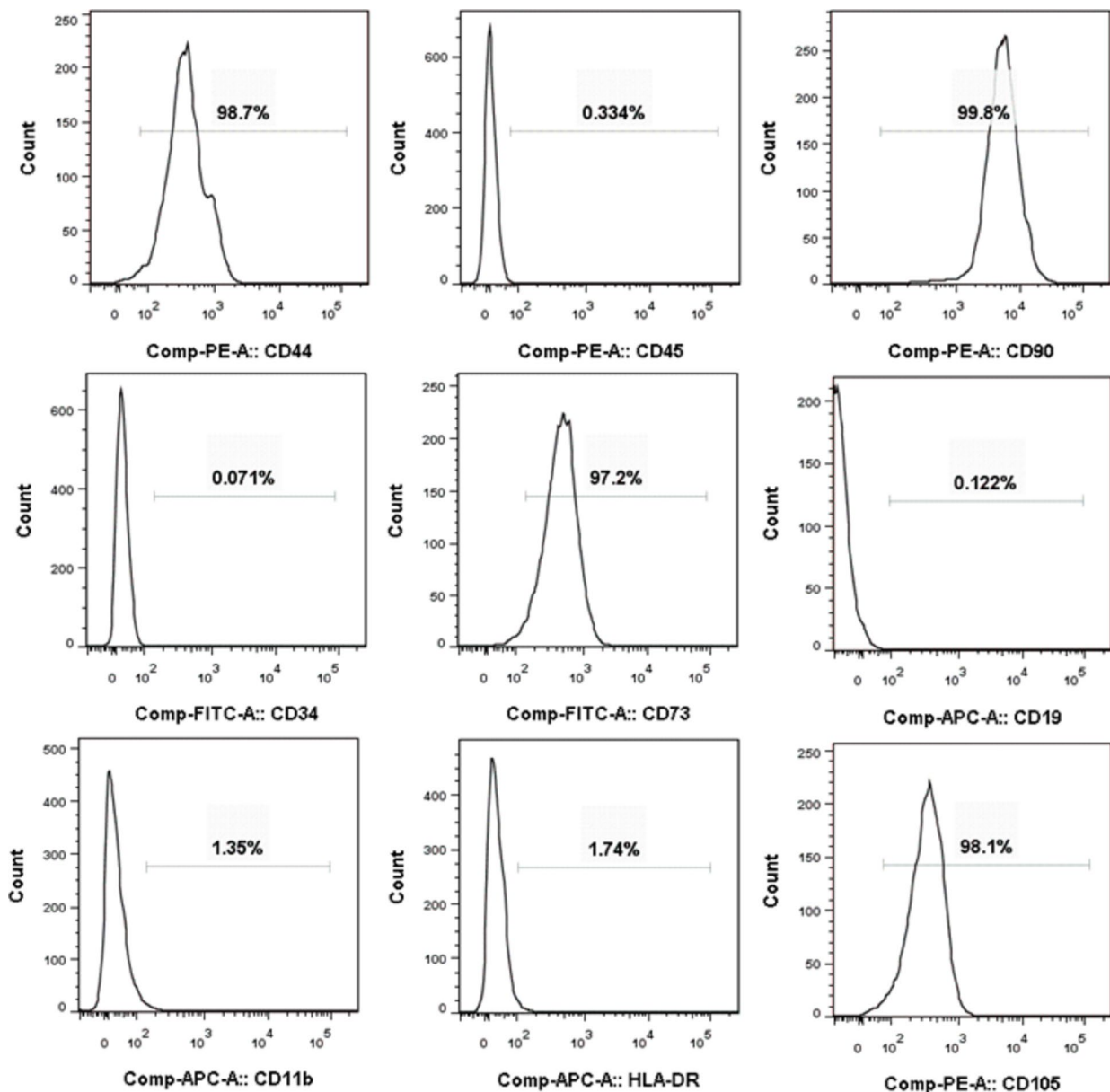


Fig. 2 Identification of surface markers of hUC-MSCs. Flow cytometry was used to determine surface marker expression, including CD44, CD45, CD90, CD34, CD73, CD19, CD11b, HLA-DR and CD105

Assessment of Urinary Protein in Mice

Urine samples were collected from the mice every two weeks over a 24-hour period to assess urinary protein levels. Urinary protein concentrations were measured using the Coomassie Brilliant Blue (CBB) method, following the instructions provided with the urinary protein detection kit (Jiancheng, Nanjing, China).

Hematoxylin-Eosin (HE) Staining

Kidney tissues from mice were excised and washed with PBS, followed by fixation in 4% paraformaldehyde for 24 h. After paraffin embedding and sectioning, the samples were subjected to HE staining. The sections were then mounted with neutral gum and examined under an optical microscope to assess the pathological morphological characteristics of the kidneys.

Isolation of CD4⁺ T Lymphocytes from Mouse Spleen

Mouse spleens were harvested and gently crushed using a 10 ml syringe plunger to prepare a single-cell suspension, followed by filtration through a 70 µm cell strainer to remove debris then the suspension was centrifuged at 500 g for 7 min at 4 °C. The supernatant was discarded and 5 ml of erythrocyte lysis buffer (Solarbio, Beijing, China) was added to lyse the erythrocytes. The mixture was gently vortexed before standing for 5 min at room temperature and the lysis reaction was terminated by the addition of 10 ml of PBS. Further, a second centrifugation was conducted as before and the supernatant was discarded. The white cell pellet was washed with PBS and resuspended in complete RPMI 1640 medium. CD4⁺ T lymphocytes were then isolated using a cell separation magnet (BD Biosciences, San Jose, CA, USA).

Western Blot (WB)

Cells were collected, and total protein was extracted using RIPA lysis buffer (Solarbio, Beijing, China) and was quantified using a Bradford protein concentration assay kit (BOSTER, Wuhan, China). The total protein was separated on a 10% gel using SDS-PAGE, and the separated proteins were transferred to a PVDF membrane (Millipore, USA). The membranes were blocked with 5% nonfat milk for 1 h at room temperature. The transferred PVDF membrane was then incubated with primary antibodies against Glucose transporter type 1 (GLUT1), hexokinase 2 (HK2), phosphofructokinase-1 (PFK-1), lactate dehydrogenase A (LDHA), Janus kinase (JAK)1, p-JAK1, signaling transducers and transcriptional activator (STAT)1, p-STAT1, PI3K, and Akt, and gently shaken overnight at 4 °C. The membranes were subsequently incubated with the appropriate secondary antibodies for 1.5 h at room temperature. Finally, the membrane was treated with an enhanced chemiluminescence detection kit (Vazyme, Nanjing, China) to visualize the WB bands.

Statistical Analysis

Energy metabolism data analyses were conducted using Wave software and GraphPad Prism 10.0 software was used for statistical analyses. Count data were presented as percentages (%) and analyzed using either χ^2 chi-squared test or Fisher's exact probability method. Measurement data were expressed as $\bar{X} \pm S$ or M(P25,P75). Student's t test or Mann-Whitney U test was performed between the two groups. For comparisons among multiple groups, one-way analysis of variance or the Kruskal-Wallis test was performed. *P* values <0.05 were considered statistically significant.

Results

Clinical Characteristics of SLE Patients

A total of 15 treatment-naïve SLE patients (12 females and 3 males) within 1 year were enrolled in this study. The mean age of the cohort was 29.3 ± 9.9 years with a mean disease duration of 5.0 ± 3.9 months. Among these patients, 7 (46.7%) exhibited a rash, 7 (46.7%) had joint involvement, 3 (20%) presented with neurological symptoms, 4 (26.7%) showed signs of serositis, 5 (33.3%) had renal involvement, 4 (26.7%) exhibited leukopenia, 5 (33.3%) had anemia, 7 (46.7%) presented with thrombocytopenia, 12 (80.0%) tested positive for anti-ds-DNA antibodies, and 14 (93.3%) demonstrated low levels of complement C3 or C4. The SLEDAI-2 K score was 10.8 ± 5.0 (Table 1).

Increased Levels of Glucose Metabolism in CD4⁺ T Cells in SLE Patients

Overactivated CD4⁺ T cells in the peripheral blood of SLE patients contribute to the differentiation and proliferation of these cells. To investigate whether energy metabolism is altered after activation of CD4⁺ T cells in SLE patients, we examined OCR and glycoPER of peripheral blood CD4⁺ T cells in the patients and healthy controls (Fig. 3a and e). The real-time mitochondrial pressure assay revealed that the basal and maximal respiration rates of CD4⁺ T cells in

Table 1 Baseline clinical characteristics of SLE patients and healthy control

Basic characteristics	SLE(<i>n</i> =15)	Healthy control(<i>n</i> =15)
Age, mean±SD, years	29.3±9.9*	31.8±4.9
Female, <i>n</i> (%)	12(80.0%)*	12(80.0%)
BMI, mean±SD, kg / m ²	22.3±2.4*	21.9±1.8
duration of illness, mean±SD, months	5.0±3.9	--
rash, <i>n</i> (%)	7(46.7%)	--
arthritis, <i>n</i> (%)	7(46.7%)	--
neurological involvement, <i>n</i> (%)	3(20.0%)	--
serositis, <i>n</i> (%)	4(26.7%)	--
renal involvement, <i>n</i> (%)	5(33.3%)	--
leukopenia, <i>n</i> (%)	4(26.7%)	--
anemia, <i>n</i> (%)	5(33.3%)	--
thrombocytopenia, <i>n</i> (%)	7(46.7%)	--
low complement C3 or C4, <i>n</i> (%)	14(93.3%)	--
ds-DNA positive, <i>n</i> (%)	12(80.0%)	--
SLEDAI-2 K score, mean±SD	10.8±5.0	--
≤6, <i>n</i> (%)	3(20%)	--
7–12, <i>n</i> (%)	6(40%)	--
≥12, <i>n</i> (%)	6(40%)	--

BMI body mass index, ds-DNA anti-double-stranded DNA, SLEDAI-2K SLE Disease Activity Index-2000

**P*>0.1 Compared to healthy controls

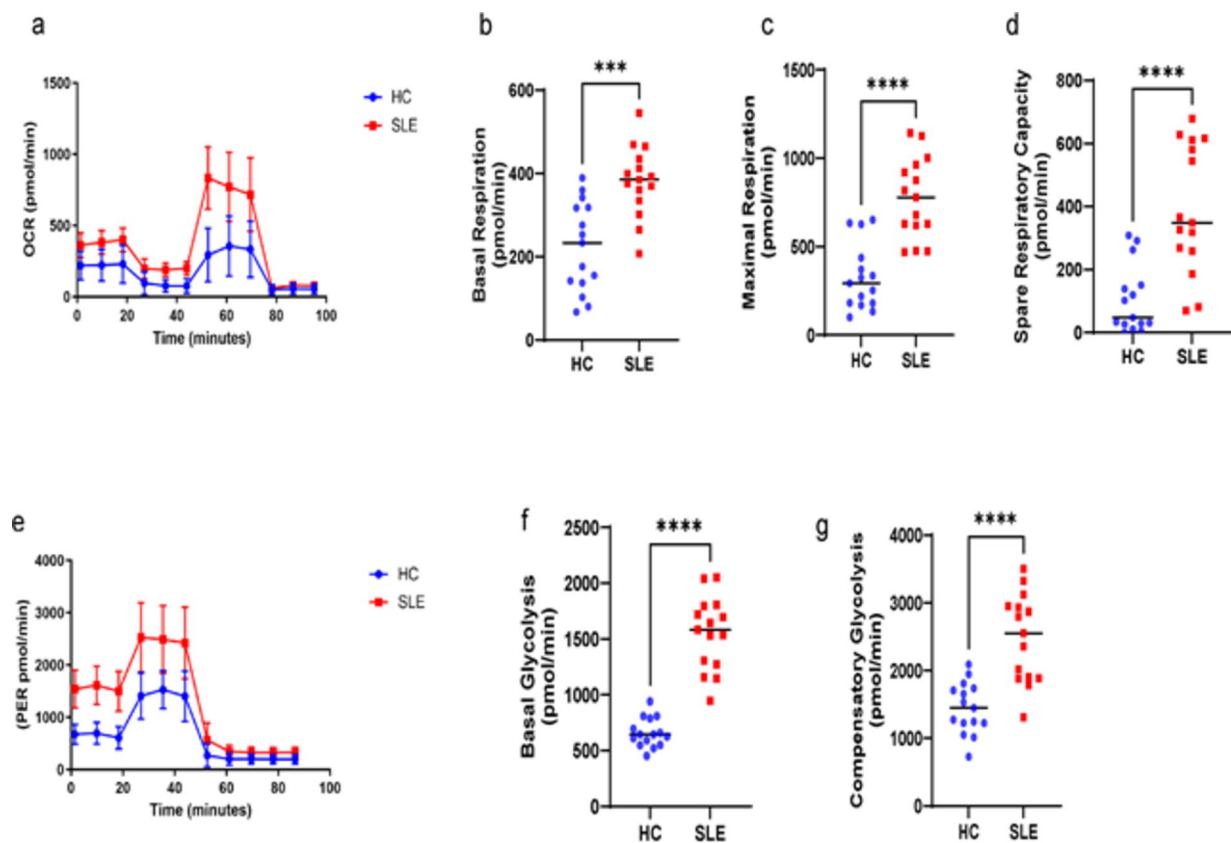


Fig. 3 Glucose metabolism levels of CD4⁺ T cells from SLE patients were significantly higher than those of healthy controls. **(a)** Mitochondrial stress test curve depicts the OCR changes over time. **(b)** Basal respiration, energy requirements of the cell under basal conditions. **(c)** Maximal respiration, representing the highest rate of oxygen consumption after adding the uncoupler FCCP. **(d)** Spare respiratory capacity

SLE patients were significantly higher than those in healthy controls (381.2 ± 83.9 vs. 223.4 ± 107.6 pmol/min, $P < 0.001$; 773.4 ± 227.9 vs. 327.3 ± 184.9 pmol/min, $P < 0.0001$, respectively, Fig. 3b and c). The spare respiratory capacity (SRC), defined as the difference between maximal and basal OCR, was also markedly higher in SLE patients compared to healthy controls ($348.4(259.3, 611.0)$ vs. $47.4(26.7, 150.9)$ pmol/min, $P < 0.0001$, Fig. 3d). In the glycolysis rate assay, both basal glycolysis and compensatory glycolysis levels of CD4⁺ T cells were substantially elevated in SLE patients compared to healthy controls (1549 ± 326.7 vs. 659.9 ± 129.9 pmol/min, $P < 0.0001$; 2480 ± 654.1 vs. 1446 ± 380.3 pmol/min, $P < 0.0001$, respectively, Fig. 3f and g). Moreover, the levels of oxidative phosphorylation (OXPHOS) and glycolysis of CD4⁺ T cells in SLE patients were increased, suggesting that abnormal glucose metabolism of CD4⁺ T cells may contribute to the pathogenesis of SLE.

To validate the above metabolic profile, we collected CD4⁺ T cell culture supernatants from SLE patients and healthy controls to measure glucose and lactate levels. This experiment showed that the glucose levels of SLE

reflects a cell's ability meeting increased energy demand. **(e)** Glycolysis rate test curve shows the PER over time. **(f)** Basal glycolysis, indicating the baseline glycolytic activity. **(g)** Compensatory glycolysis, indicating the glycolytic response to the increased energy demand. ($n = 15$ per group) (All experiments were repeated three times). (** $P < 0.001$; **** $P < 0.0001$)

patients were substantially lower than those of healthy controls (9.89 ± 1.68 vs. 12.85 ± 3.39 mmol/L, $P = 0.0053$, Fig. 4a). The lactate levels of SLE patients were significantly higher than those of healthy controls (8.827 ± 2.092 vs. 4.787 ± 1.218 mmol/L, $P < 0.0001$, Fig. 4b).

hUC-MSCs Inhibited the Proliferation of CD4⁺ T Cells in SLE Patients

As described above, MSCs have immunomodulatory effects, but the specific immunological mechanisms have not been elucidated. To investigate the immunomodulatory effect of hUC-MSCs on peripheral blood CD4⁺ T cells from patients with SLE, we assessed CD4⁺ T cell proliferation after 72 h of co-culture with hUC-MSCs at different ratios (50:1, 10:1, and 5:1), as well as in cultures without hUC-MSCs. The results indicated that cell viability varied across groups, with the viability of CD4⁺ T cells at the 10:1 and 5:1 ratios being markedly lower than that of the CD4⁺ T cell-only group ($P < 0.0001$, Fig. 5). Conversely, no significant difference was observed between 10:1 and 5:1 groups

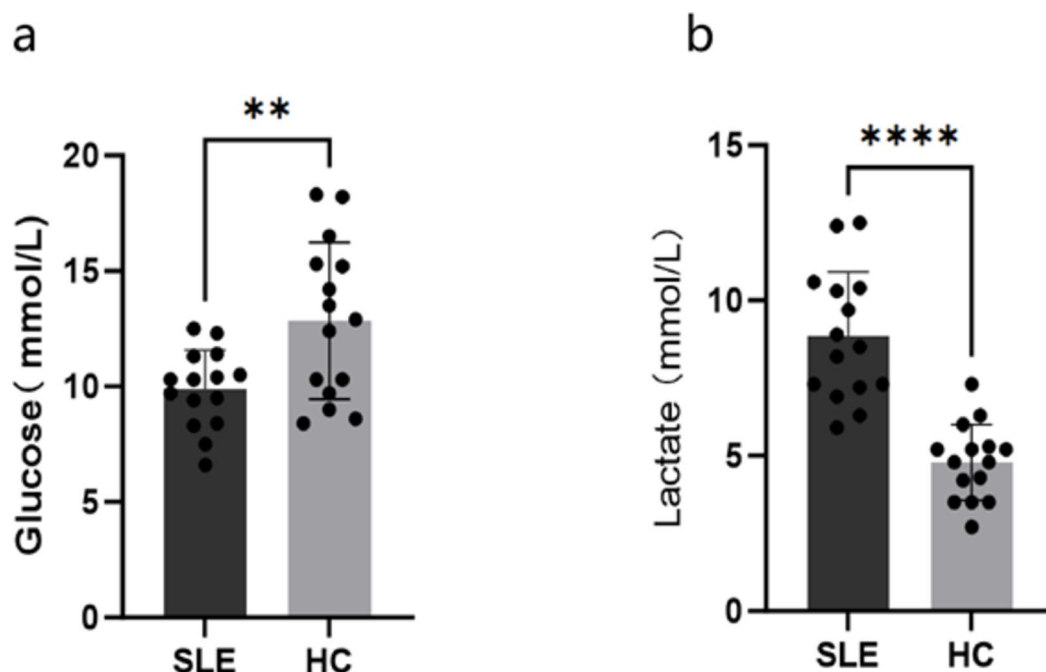


Fig. 4 Glucose and lactate levels of CD4⁺ T cell culture supernatant in SLE patients and normal controls. **(a)** The glucose levels of SLE patients were significantly lower than those of healthy controls. **(b)**

The lactate levels in SLE patients were significantly higher than those in healthy controls. ($n=15$ per group) (** $P<0.01$; **** $P<0.0001$)

($P>0.05$), suggesting that hUC-MSCs substantially inhibited the proliferation of SLE-CD4⁺ T cells within a specific ratio range. Due to the limited density of MSCs, we selected a ratio of 10:1 (CD4⁺ T cells: MSCs) for subsequent studies.

hUC-MSCs Reduced the High Glucose Metabolism Levels of SLE-CD4⁺ T Cells

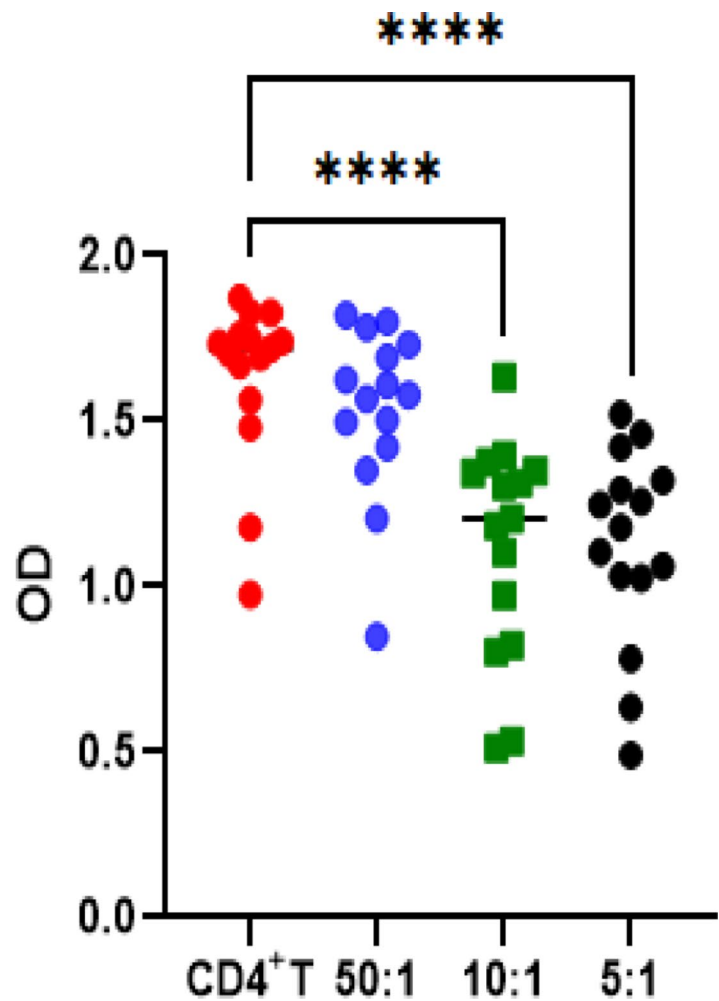
To further investigate the effects of hUC-MSCs on the metabolic profile of SLE-CD4⁺ T cells, we co-cultured SLE-CD4⁺ T cells with hUC-MSCs at a ratio of 10:1 and using only SLE-CD4⁺ T cells as a control. Mitochondrial respiration and glycolysis rates were measured after 72 h of culture (Fig. 6a and e). Our results indicate that CD4⁺ T cells co-cultured with hUC-MSCs did not show significant differences in basal respiration compared to controls (Fig. 6b); however, maximal respiration was considerably lower in the co-cultured group (437.3 ± 155 vs. 761.4 ± 213.1 pmol/min, $P<0.0001$, Fig. 6c). Also, the spare respiratory capacity of CD4⁺ T cells was substantially decreased after co-culture with hUC-MSCs ($366.1(326.1, 611.0)$ vs. $29.14(22.2, 71.1)$ pmol/min, $P<0.0001$, Fig. 6d), indicating that mitochondrial OXPHOS levels of SLE-CD4⁺ T cells decreased after the co-culture. Compared to the control group, both basal and compensatory glycolysis levels were markedly reduced in CD4⁺ T cells co-cultured with hUC-MSCs (690.6 ± 170.9 vs. 1679 ± 192.9 pmol/min, $P<0.0001$; $1532(1358, 1707)$ vs. $2968(2872, 3126)$ pmol/min, $P<0.0001$, respectively).

Figure 6f and g), suggesting that co-culture with hUC-MSCs alleviated the abnormally elevated glucose metabolism levels in SLE-CD4⁺ T cells.

Effect of hUC-MSCs on the Levels of Supernatant Cytokines in SLE-CD4⁺ T Cells

The proliferation, activation, and differentiation of CD4⁺ T cells are accompanied by the production of a large number of cytokines. To further understand the effect of hUC-MSCs on SLE-CD4⁺ T cells, we collected culture supernatants from the two groups for multiplex cytokine detection by flow cytometry. Compared to the control group, hUC-MSCs markedly inhibited the release of interferon-gamma (IFN- γ), interleukin (IL)-17, and tumor necrosis factor-alpha (TNF- α) in the supernatant of SLE-CD4⁺ T cells ($P<0.01$), while the levels of IL-4 and IL-10 were increased ($P<0.0001$) (Fig. 7; Table 2). T helper (Th)1 cells mainly secrete (IFN)- γ , Th2 cells express IL-4, IL-5, and IL-6, Th17 cells produce IL-17, and Treg cells mainly produce IL-10. The current results showed that proinflammatory cytokines are down-regulated in SLE-CD4⁺ T cells after co-culture with hUC-MSCs, while anti-inflammatory cytokines were drastically increased in SLE-CD4⁺ T cells with the co-culture. These changes may be associated with hUC-MSCs promoting the differentiation of CD4⁺ T cells into various subsets, particularly affecting the Th1/Th2 and Th17/Treg ratios. Furthermore, the T cell subsets have different glucose metabolism

Fig. 5 hUC-MSCs substantially inhibited the proliferation of SLE-CD4⁺ T cells within a specific ratio range. The proliferation of CD4⁺ T cells was measured after 72 h co-culture with hUC-MSCs in vitro via transwell technique at different ratios (50:1, 10:1, 5:1) by CCK-8 assay. ($n=15$ per group) (**** $P<0.0001$)



patterns, demonstrating unique metabolic phenotypes that need to be substantiated by subsequent in vitro experiments.

Transcriptomics

To further understand the effect of hUC-MSCs at the gene level of SLE-CD4⁺ T cells, we conducted transcriptomic analysis to evaluate the differences in mRNA expression between the two groups. Total RNA was extracted from SLE-CD4⁺ T cells in the two groups. The sequencing results of all samples were high-quality and had a balanced base distribution. RNA-sequencing produced an average of 50 million raw reads. The differential expression of genes between the two groups was analyzed using the R software package DESeq2, and the default screening threshold for DEGs was $|\log_2FC| > 1$ and $P_{adj} < 0.05$. A total of 60,693 genes were analyzed, resulting in the identification of 606 differential genes. Among these, the mRNA levels of 434 genes were upregulated, while 172 genes were downregulated (Fig. 8a). To further visualize these differential genes, we conducted volcano map and hierarchical clustering heatmap analyses

(Fig. 8b and c). Among these, the top five downregulated genes were *GJB2*, *IL1R1*, *TNFSF14*, *NPTX1*, and *NEK6*, while the top five upregulated genes were *ALDOC*, *ID3*, *HIC1*, *SMOX*, and *TNFRSF18*.

Kyoto Encyclopedia of Genes and Genomes (KEGG) pathway enrichment and Gene Ontology (GO) analyses were performed for DEGs (Fig. 8d and e). KEGG pathway enrichment analysis showed that DEGs were mainly enriched in cytokine-cytokine receptor interaction, virus protein-cytokine and cytokine-receptor interaction, JAK-STAT pathway, hematopoietic cell lineage, chemokine pathway, amino acid biosynthesis, PI3K-Akt pathway, butyrate metabolism, and others. GO analysis showed that biological processes mainly included viral response, viral genome replication defense response, viral immune response, chemokine-mediated signaling pathway, inflammatory response, negative regulation of cell proliferation, IFN- β production, positive regulation of JAK-STAT cascade, and positive regulation of cytosolic calcium ion concentration. Cellular component included the cytoplasmic membrane, extracellular region, extracellular space

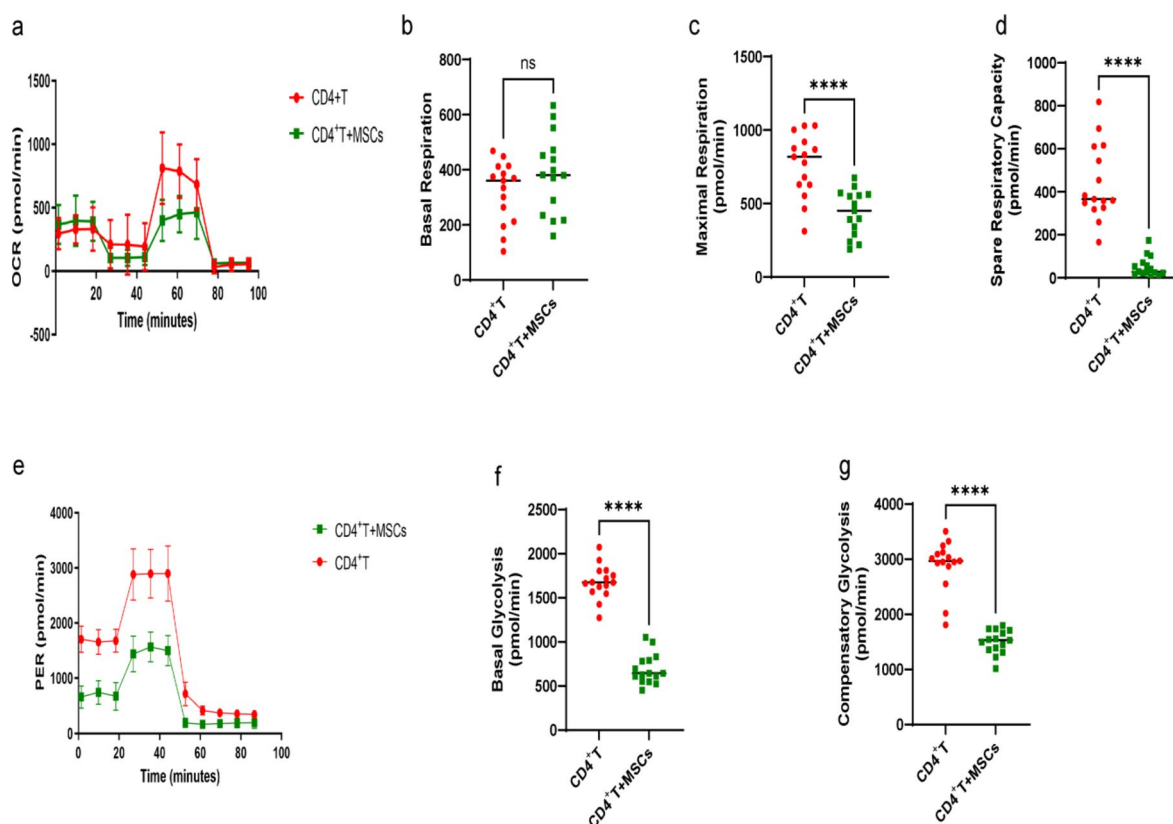


Fig. 6 hUC-MSCs improved the abnormally elevated glucose metabolism levels in SLE-CD4⁺ T cells. Real-time measurements of mitochondrial stress and glycolytic rate for only CD4⁺ T and CD4⁺ T+MSCs groups (CD4⁺ T cells and hUC-MSCs at a 10:1 ratio). **(a)** The curve of the mitochondrial stress test. **(b)** CD4⁺ T cells co-cultured with hUC-MSCs did not differ significantly from controls in basal respiration. **(c)** CD4⁺ T cells co-cultured with hUC-MSCs had significantly

lower maximal respiration than that in the control group. **(d)** The spare respiratory capacity of CD4⁺ T cells was substantially decreased after co-culture with hUC-MSCs. **(e)** The curve of the glycolysis rate test. Compared to the control group, the levels of basal **(f)** and compensatory glycolysis **(g)** were decreased significantly in CD4⁺ T cells co-cultured with hUC-MSCs. ($n=15$ per group) (**** $P<0.0001$)

outside of the plasma membrane, components of the plasma membrane, endoplasmic reticulum lumen, and perinucleus region of the cytoplasm. Molecular function mainly included cytokine activity, 2'-5'-oligopoly adenylyl synthase activity, double-stranded RNA binding, cytokine binding, monocarboxylic acid transmembrane transporter activity, chemokine activity, same protein binding, very low-density lipoprotein particle binding, protein binding, CXCR chemokine receptor binding, and growth factor activity. The genetic analysis tool and Cytoscape software were employed to construct the protein-protein interaction network (PPI) of DEGs, followed by molecular screening to identify the hub genes (Fig. 9a and b). Among these, *VEGFA*, *IL-10*, *HSP90AA1*, *IFNB1*, *F2R*, and *NR4A1* were related to the JAK-STAT and PI3K-Akt pathways. q-PCR validation results showed that after cocultured with hUC-MSCs, CD4⁺ T cells exhibited upregulated genes of *VEGFA*, *IFNB1*, and *NR4A1*, followed with downregulated

genes of *IL-10*, *HSP90AA1* and *F2R*, which were consistent with the sequencing results (Fig. 10; Table 3).

hUC-MSCs Alleviate Disease Manifestations in MRL/lpr Mice

To further investigate the effects of hUC-MSCs on SLE, we administered 8×10^5 hUC-MSCs via tail vein injection to the mice of SLE+MSCs group at 16 weeks of age, while the mice of SLE+PBS group and control group were received an equivalent volume of PBS. A second injection of the same dosage was administered at 18 weeks (Fig. 11a). Skin lesions were first observed in mice of SLE+PBS and SLE+MSCs groups at 15 weeks. By 20 weeks, the mice of SLE+PBS group exhibited pronounced skin lesions, while the SLE+MSCs group demonstrated a modest reduction in lesion severity (Fig. 11b). The SLE+PBS group mice showed marked splenic enlargement compared to the control

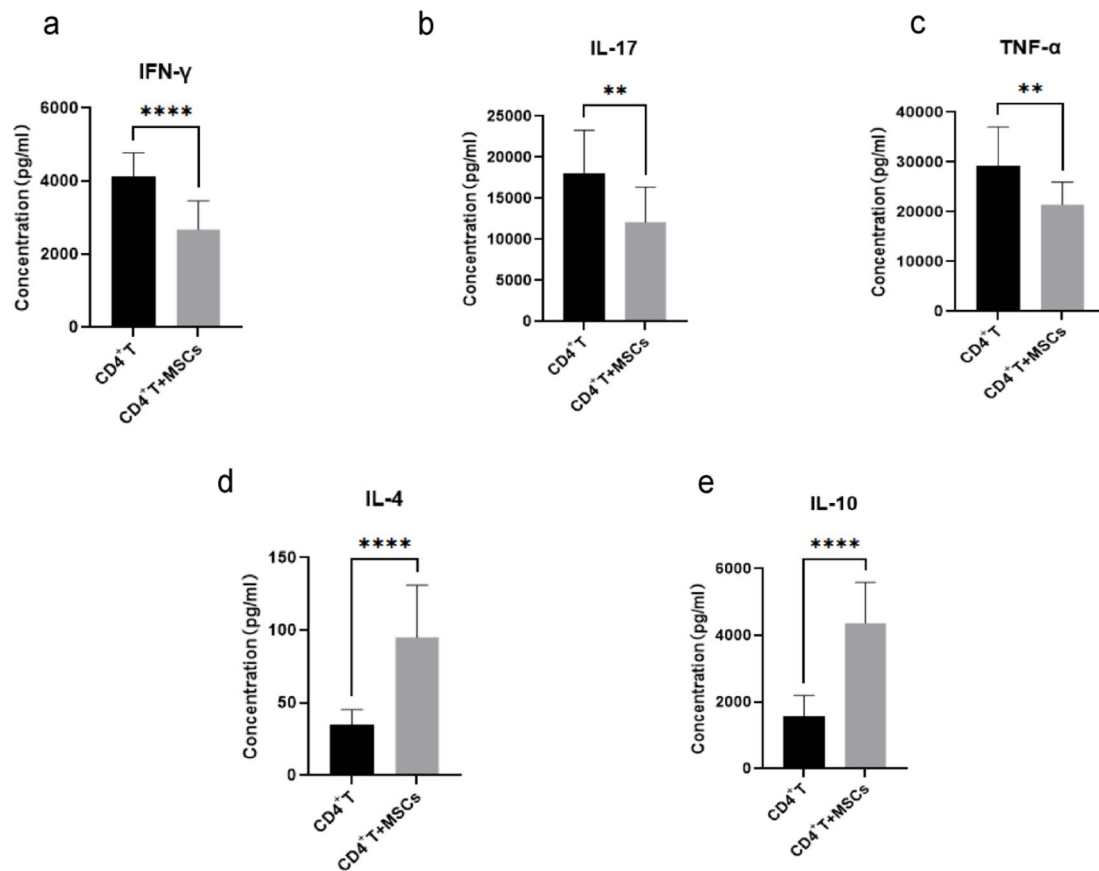


Fig. 7 Effect of hUC-MSCs on the levels of supernatant cytokines in SLE-CD4⁺ T cells. CD4⁺ T cells from SLE patients were co-cultured with hUC-MSCs at a ratio of 10:1 for 72 h. Compared to the control

group, hUC-MSCs inhibited the release of IFN-γ, IL-17, and TNF-α in the supernatant of SLE-CD4⁺ T cells, while the levels of IL-4 and IL-10 were increased. ($n=15$ per group) (** $P<0.01$; **** $P<0.0001$)

group, whereas the mice of SLE+MSCs group exhibited reduced splenomegaly (Fig. 11c). Regarding renal injury, urinary protein levels in mice of the SLE+MSCs group were significantly lower than those in the SLE+PBS group at both 18 and 20 weeks ($P<0.01$, Fig. 11d). HE staining revealed varying degrees of alleviation in inflammatory cell infiltration and mesangial cell proliferation in the kidneys of the mice in SLE+MSCs group compared to the SLE+PBS group (Fig. 11e). These findings provide evidence that hUC-MSCs can mitigate the immune-mediated organs injury in MRL/lpr mice.

Table 2 Cytokines in culture supernatants between the two groups

Cytokines (pg/mL)	CD4 ⁺ T ($n=15$)	CD4 ⁺ T+MSCs ($n=15$)	P value
IFN-γ	3995(3521,4772)	2623(2144,2745)	<0.0001
IL-17	18,124±5185	12,087±4286	0.0017
TNF-α	29,258±7799	21,421±4550	0.0023
IL-4	34.87±10.36	95.05±35.95	<0.0001
IL-10	1583±614.50	4361±1228	<0.0001

IFN-γ interferon-gamma, IL interleukin, TNF-α tumor necrosis factor-alpha, MSCs mesenchymal stem cells

hUC-MSCs Inhibited the Expression of Glucose Metabolism Related Enzymes, as well as the JAK-STAT and PI3K-Akt Signaling Pathways in CD4⁺ T Lymphocytes of MRL/lpr Mice

GLUT1, HK2, PFK-1, and LDHA are key enzymes in glucose metabolism. To investigate glucose metabolism in mouse splenic CD4⁺ T lymphocytes, we assessed the protein expression of these glucose metabolism related enzymes. The results indicated that the protein expression levels of GLUT1, HK2, PFK-1, and LDHA were markedly higher in the SLE+PBS group compared to the control group ($P<0.01$). Conversely, the protein expression of GLUT1, HK2, PFK-1, and LDHA was substantially reduced in the SLE+MSCs group compared to the SLE+PBS group ($P<0.05$) (Fig. 12a).

To determine whether there were alterations in the JAK-STAT and PI3K-Akt signaling pathways in splenic CD4⁺ T lymphocytes following hUC-MSCs treatment, we evaluated the protein expression levels of relevant signaling components. The results demonstrated that the protein expression levels of p-JAK1/JAK1, p-STAT1/STAT1, PI3K, and Akt

a Statistic of Differently Expressed gene

Differently Expressed gene number

Type

- Up
- Down

b Volcano Plot: $q\text{-value} < 0.05$ & $\log_2FC > 1$

$q\text{-value} < 0.05$ & $\log_2FC > 1$

c

Group

- Group 1
- Group 2
- Group 3
- Group 4
- Group 5
- Group 6
- Group 7
- Group 8
- Group 9
- Group 10
- Group 11
- Group 12
- Group 13
- Group 14
- Group 15
- Group 16
- Group 17
- Group 18
- Group 19
- Group 20
- Group 21
- Group 22
- Group 23
- Group 24
- Group 25
- Group 26
- Group 27
- Group 28
- Group 29
- Group 30
- Group 31
- Group 32
- Group 33
- Group 34
- Group 35
- Group 36
- Group 37
- Group 38
- Group 39
- Group 40
- Group 41
- Group 42
- Group 43
- Group 44
- Group 45
- Group 46
- Group 47
- Group 48
- Group 49
- Group 50
- Group 51
- Group 52
- Group 53
- Group 54
- Group 55
- Group 56
- Group 57
- Group 58
- Group 59
- Group 60
- Group 61
- Group 62
- Group 63
- Group 64
- Group 65
- Group 66
- Group 67
- Group 68
- Group 69
- Group 70
- Group 71
- Group 72
- Group 73
- Group 74
- Group 75
- Group 76
- Group 77
- Group 78
- Group 79
- Group 80
- Group 81
- Group 82
- Group 83
- Group 84
- Group 85
- Group 86
- Group 87
- Group 88
- Group 89
- Group 90
- Group 91
- Group 92
- Group 93
- Group 94
- Group 95
- Group 96
- Group 97
- Group 98
- Group 99
- Group 100

d Top 19 of Enrichment

Top 19 of Enrichment

Gene Number

- 4
- 10
- 31

$p\text{-value}$

- 0.08
- 0.06
- 0.04
- 0.02

e Top GO Term

Top GO Term

$-\log_{10} p\text{-value}$

biological process

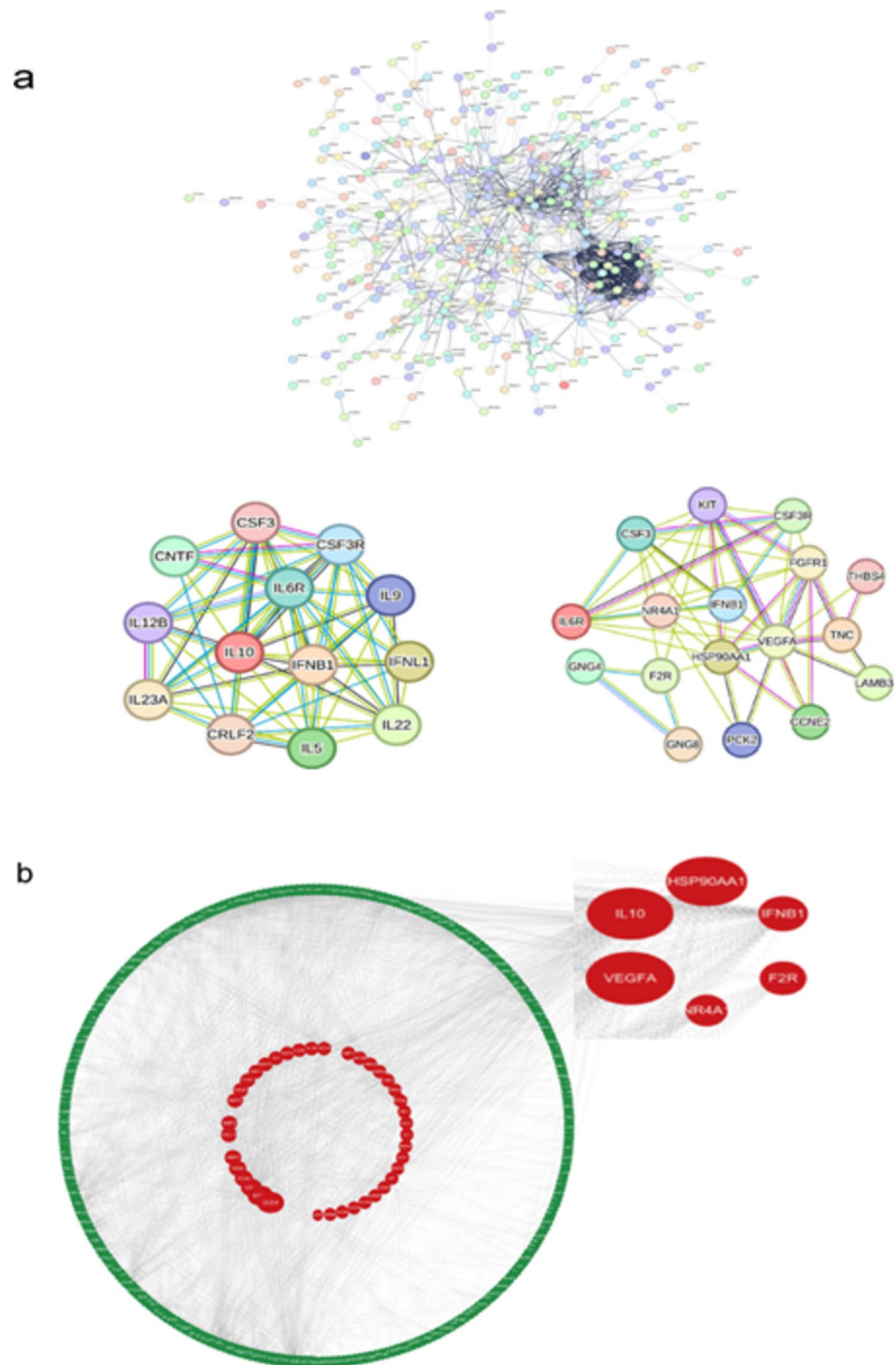
cellular component

molecular function

Discussion

This study shows that levels of glycolysis and oxidative phosphorylation in CD4⁺ T cells were considerably elevated in SLE patients. hUC-MSCs decreased the proliferative activity, altered the glucose metabolism phenotype, reduced

Fig. 9 Using STRING database and Cytoscape software to construct PPI and identify hub genes. The genetic analysis tool and Cytoscape software were used to construct the PPI (a) of DEGs, followed by molecular screening to identify the hub genes (b). Among these, *VEGFA*, *IL-10*, *HSP90AA1*, *IFNB1*, *F2R*, and *NR4A1* were related to the JAK-STAT and PI3K-Akt pathways



pro-inflammatory factor levels, and increased anti-inflammatory factor levels in SLE CD4⁺ T cells. The regulatory effects of hUC-MSCs on the cellular energy metabolism phenotype may be related to the influence of JAK-STAT and PI3K-Akt signaling pathways. Our study investigates the relationship between immune regulatory mechanisms and glucose metabolism profiles, as well as the role of hUC-MSCs in the treatment of SLE. It may reveal the

pathogenesis of SLE and provide novel strategies for individualized precision treatment.

The activation and proliferation of T cells require substantial upregulation of energy metabolism to induce and maintain an immune response [22]. Glucose is the primary source of energy supply, mainly through aerobic oxidation, anaerobic glycolysis, and pentose phosphate pathway [23]. T cells in SLE exhibit heightened activity and demonstrate

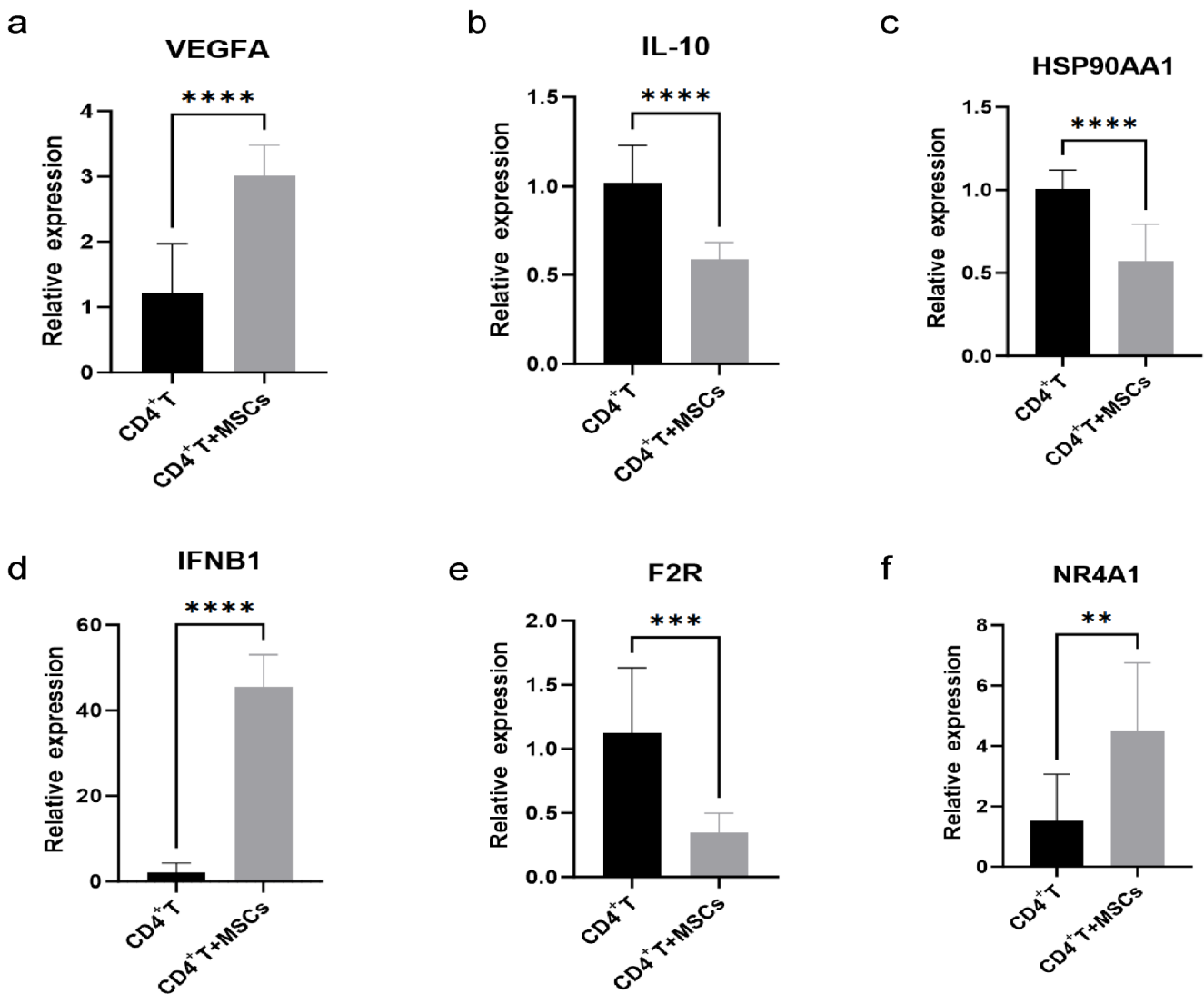


Fig. 10 The key genes including *VEGFA* (a), *IL-10* (b), *HSP90AA1* (c), *IFNB1* (d), *F2R* (e), and *NR4A1* (f) were normalized and validated by q-PCR, and the validation results were consistent with the sequencing results. (** $P < 0.01$; *** $P < 0.001$; **** $P < 0.0001$)

Table 3 Relative expression of genes between the two groups

Genes	CD4 ⁺ T	CD4 ⁺ T+MSCs	P value
<i>VEGFA</i>	2.74±1.91	6.82±1.07	0.0322
<i>IL-10</i>	0.96±0.22	0.55±0.10	0.0436
<i>HSP90AA1</i>	1.09±0.19	0.52±0.15	0.0171
<i>IFNB1</i>	17.81±9.35	342.00±180.00	0.0357
<i>F2R</i>	1.24±0.33	0.20±0.10	0.0070
<i>NR4A1</i>	1.06±0.59	12.81±3.92	0.0068

MSCs mesenchymal stem cells

abnormalities across various metabolic pathways, including glycolysis, oxidative stress, and mammalian target of rapamycin (mTOR) pathway [24]. In the present study, the basal glycolysis, compensatory glycolysis, basal respiration, maximal respiratory capacity, and spare respiratory capacity of CD4⁺ T cells in SLE patients were markedly elevated compared to those of healthy controls, indicating

that their glycolytic and OXPHOS levels were higher than in the healthy control group. Furthermore, measurements of glucose and lactate levels in cell culture supernatants confirmed a considerable increase in glucose uptake and metabolism, particularly glycolysis, in SLE-CD4⁺ T cells.

Naive T cells have relatively low energy requirements and minimal glucose intake [25]. After activation, T cells rapidly undergo proliferation and differentiation [22]. In SLE, activation of CD4⁺ T cells induces the T cell receptor and co-stimulatory receptors (such as CD28) to upregulate glucose transporter 1 through the PI3K-Akt pathway. This signaling cascade, mediated by the transcription factor Myc, further promotes the expression of glycolytic enzymes, thereby enhancing glycolysis and supplying the energy required for T cell growth and proliferation [26]. Chronic activation of T cells in both SLE patients and mouse models is associated

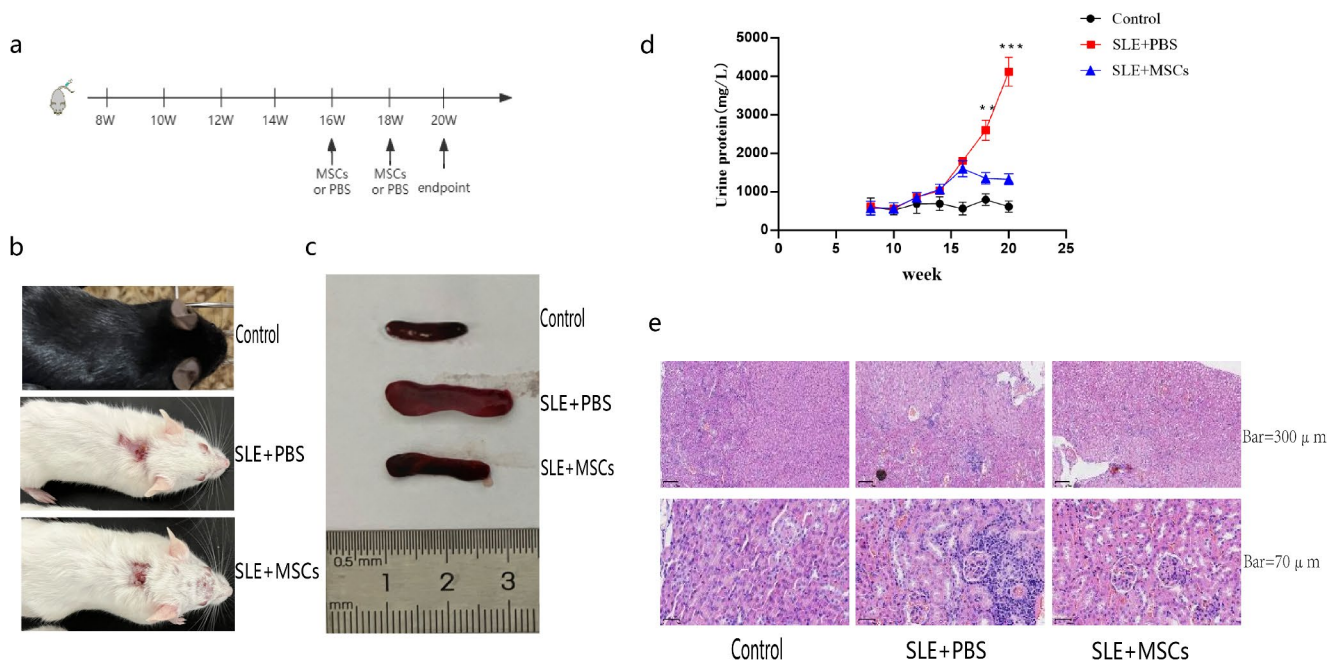


Fig. 11 hUC-MSCs alleviate disease manifestations in MRL/lpr mice. **(a)** Flowchart depicting the animal experiments. **(b)** Skin lesions in mice of different groups at 20 weeks. **(c)** Spleen morphology in the various groups of mice at 20 weeks. **(d)** Changes in urinary protein levels from week 8 to week 20. At weeks 18 and 20, a statistically

significant difference in urinary protein was observed between the SLE+PBS and SLE+MSCs groups ($n=3$ per group) (** $P<0.01$; *** $P<0.001$). **(e)** Representative images of kidney sections stained with HE. Scale bars: 300 μ m and 70 μ m

with elevated glycolytic rates and increased glycolytic flux [27]. Moreover, the degree of glycolytic dependence varies among different T cell subsets. Th17 and Th1 cells derived from CD4⁺ T cells provide the energy required for cell proliferation and function via glycolysis pathway, while Treg and memory T cells supply the energy required by fatty acid oxidation and OXPHOS [28]. Th17/Treg cell balance is closely related to the development of SLE, and changes in the metabolic levels, such as abnormal glycolysis in SLE-CD4⁺ T cells, promote the differentiation and function of Th17 cells, which is the cause of Th17/Treg cell imbalance [29]. Inhibition of glycolytic pathway inhibits the differentiation of Th1, Th17, and Thf cells, promotes the proliferation and differentiation of Treg cells, restores the balance of Th17/Treg cells, and induces immune tolerance to treat SLE [30]. Furthermore, the glucose metabolism of SLE-CD4⁺ T cells also included markedly increased levels of OXPHOS. This result showed that the OCR of SLE-CD4⁺ T cells was higher than that of healthy controls, indicating enhanced oxidative phosphorylation. This upregulation is associated with the chronic activation of SLE-CD4⁺ T cells under long-term stimulation of autoantigens *in vivo* [27]. Moreover, the mitochondria of SLE-CD4⁺ T cells exhibit structural changes, including increased volume and mass, as well as hyperpolarization characterized by mitochondrial fusion and an elevated potential difference, which upregulates OXPHOS levels [31]. These findings suggest that the

energy metabolism phenotype of T cells is closely related to their proliferation and differentiation, and SLE pathogenesis is regulated by SLE-CD4⁺ T cells via metabolism. The present study establishes a correlation between energy metabolism of immune cell subsets and SLE activity, suggesting that alterations in cellular glycolysis and OXPHOS levels may serve as potential biomarkers for the clinical assessment of SLE activity [32]. Thus, targeting cellular energy metabolism phenotypes may offer new therapeutic strategies for SLE, and selective inhibitors of energy metabolism pathways could enhance the efficacy of glucocorticoids and immunosuppressants, thereby mitigating the adverse effects associated with these treatments [33].

MSCs are widely distributed in the human body, the rich sources are the umbilical cord, bone marrow, peripheral blood, placenta, adipose tissue, and dental pulp [34]. MSCs have the potential to modulate the immune system and regulate inflammation [35]. In recent years, MSCs transplantation for the treatment of autoimmune diseases, especially SLE, has gained increasing attention, and many clinical trials and animal experiments have yielded encouraging results. Treatment with MSCs can reduce the serum levels of anti-dsDNA, ANA, proteinuria, and creatinine, improve renal pathology, and alleviate inflammatory responses [36, 37]. MSCs exosomes inhibit T cell proliferation and differentiation by preventing T cells from entering the S and G0/G1 phases in a dose-dependent manner via A20 and

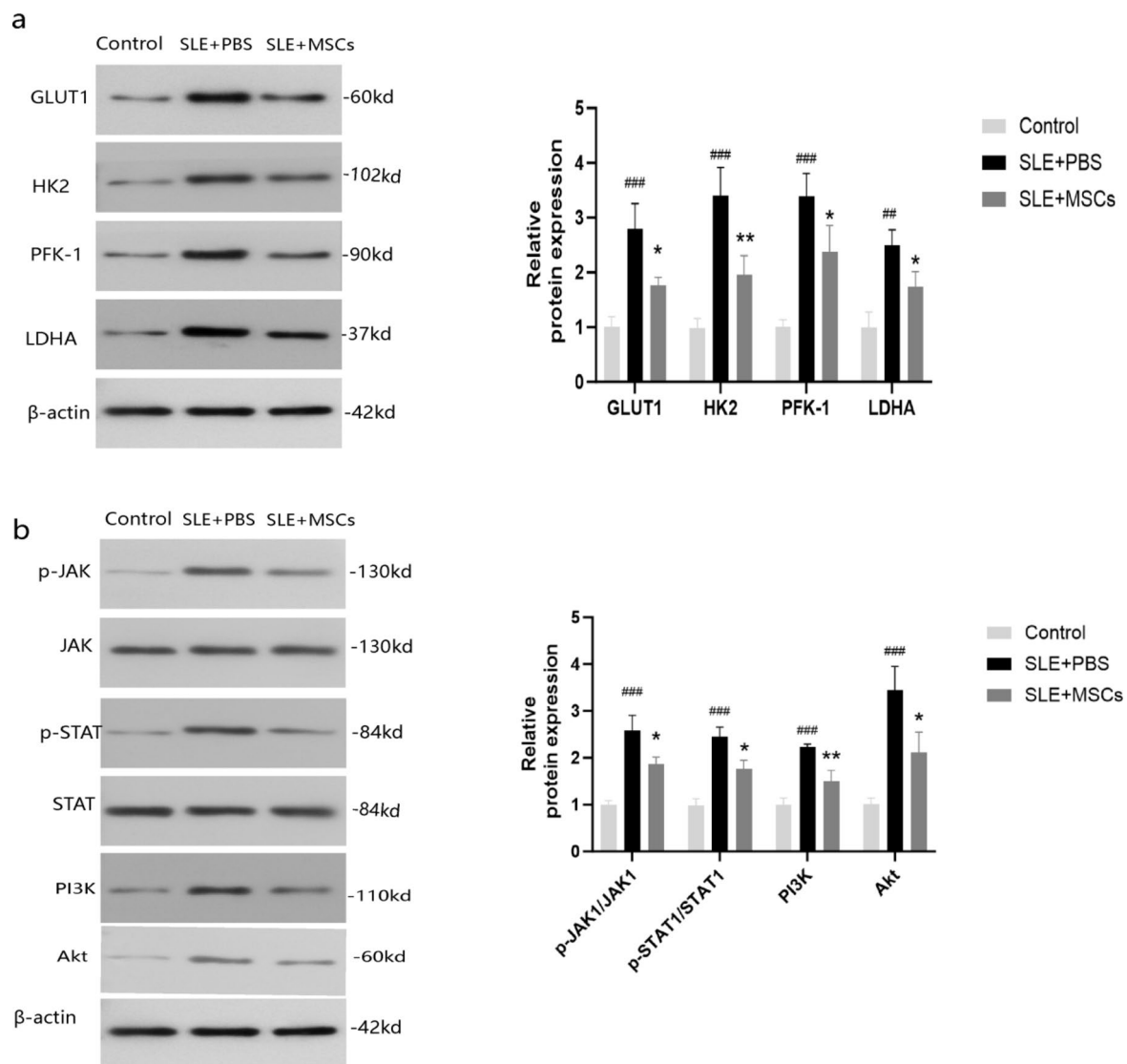


Fig. 12 hUC-MSCs inhibited the expression of glucose metabolism related enzymes, as well as the JAK-STAT and PI3K-Akt signaling pathways in CD4⁺ T lymphocytes of MRL/lpr mice. **(a)** Protein expression levels of glucose metabolism related enzymes (SLE+PBS vs. control group $##P<0.01$, $###P<0.001$; SLE+MSCs vs. SLE+PBS

group $*P<0.05$, $**P<0.01$). **(b)** Protein expression levels of the JAK-STAT and PI3K-Akt signaling pathways (SLE+PBS vs. control group $##P<0.01$, $###P<0.001$; SLE+MSCs vs. SLE+PBS group $*P<0.05$, $**P<0.01$)

TNFAIP6 [38–40]. hUC-MSCs inhibit the proliferation of CD4⁺ T cells and the production of proinflammatory cytokines in SLE while promoting the apoptosis of CD4⁺ T cells in SLE mice, inducing the differentiation of T cells from proinflammatory to anti-inflammatory, thereby alleviating SLE symptoms and improving immune imbalance [41]. Although the above studies have confirmed that hUC-MSCs have immunomodulatory effects on T lymphocytes in SLE, the specific regulatory mechanism has not been fully elucidated. In recent years, the field of energy metabolism in the mechanism of immune regulation has become a new perspective and a hot spot in the autoimmune diseases. The increasing evidence shows that the alteration of energy

metabolism process determines the proliferation, function, and differentiation of T cells. However, there are few reports on the effect of MSCs on T cell energy metabolism. Limited research shows that MSCs and vesicles can regulate Th1 cell differentiation in mice by inhibiting glycolysis [42, 43]. MSCs inhibit the mTOR pathway and regulate T cell proliferation through glycolytic conversion [44]. Nevertheless, whether MSC-mediated metabolic reprogramming affects the differentiation and function of lupus T cells as well as the detailed mechanisms, remains to be addressed.

The present study showed that co-culture with hUC-MSCs significantly decreased the proliferation viability of SLE-CD4⁺ T cells, confirming that hUC-MSCs could inhibit

the proliferation of CD4⁺ T cells in SLE patients. Furthermore, SLE-CD4⁺ T cells had a reduced glycolysis rate after co-culture with hUC-MSCs, indicating that hUC-MSCs regulate the glucose metabolism levels of SLE-CD4⁺ T cells. According to previous studies, some of the mechanisms that may be involved are as follows: (1) Differentiation of SLE-CD4⁺ T cells is abnormal, and there is an immune imbalance between the anti-inflammatory cell subsets (Treg, Th2) and pro-inflammatory cell subsets (Th17 and Th1) [45]. Pro-inflammatory T cell subsets exhibit higher glycolytic capacity [29]. Previous studies have shown that MSCs regulate T cell immunity by modulating antigen-presenting cells, promoting the expression of indoleamine 2,3-dioxygenase, prostaglandin E2, transforming growth factor-beta 1, Fas ligand, and programmed death ligand, thereby promoting the polarization of CD4⁺ T cell subsets from Th1 and Th17 to Th2 and Treg cells, respectively [46]. This study found that after co-culture with hUC-MSCs, the levels of IFN- γ and IL-17, which mainly secreted by Th1 and Th17 cells, were substantially reduced in the supernatant of SLE CD4⁺ T cell, while IL-10 and IL-4, secreted by Tregs and Th2 cells, were significantly increased. It is suggested that the effect of MSCs on CD4⁺ T cell glycolysis may be related to the inhibition of proliferation and differentiation of effector T cells such as Th1 and Th17, simultaneously the promoting of Tregs and Th2 cells. (2) Khan et al. demonstrated that TNF- α in natural killer cells promotes aerobic glycolysis via the TNF α /TNFR2 axis [47]. Our study demonstrated that co-culture with hUC-MSCs reduced the levels of TNF- α in the supernatant of SLE CD4⁺ T lymphocytes, suggesting that hUC-MSCs may inhibit glycolysis by downregulating TNF- α . (3) MSCs downregulate the levels of glycolysis affected by monocarboxylic acid transporter 4, glucose transporter 1, and glycolytic enzymes via inhibition of the expression of hypoxia-inducible factor-1 α (HIF-1 α) in the Akt/mTOR/HIF-1 α /Th17 pathway, this phenomenon has a therapeutic effect similar to sirolimus in SLE [48]. Besides, the glucose metabolism of SLE-CD4⁺ T cells performs higher levels of OXPHOS. This study suggested that after co-culture with hUC-MSCs, the levels of enhanced OXPHOS in SLE-CD4⁺ T cells decreases markedly, which might be related to hUC-MSCs-reduced chronic activation of CD4⁺ T cells, weakened mitochondrial remodeling, and inhibited mitochondrial excessive accumulation [49].

Notably, there was no migration of SLE-CD4⁺ T cells to the bottom chamber, neither MSCs-T cell interaction directly in our transwell experiment, hence it could be anticipated that the secretome from MSCs was imparting the observed influence on SLE-CD4⁺ T cells. While, the plausible candidates involved in the MSCs secretome reversing the SLE-CD4⁺ T cells' glucose metabolism deserve to be explored in our further research.

To further investigate the mechanism of the effect of hUC-MSCs on the glucose metabolism of CD4⁺ T cells in SLE patients, we conducted transcriptomic analysis on SLE-CD4⁺ T cells cultured alone and in co-culture with hUC-MSCs. This analysis revealed that differentially expressed genes were enriched in the JAK-STAT and PI3K-Akt pathways, as determined by KEGG analysis. Additionally, we conducted animal experiments, which demonstrated that hUC-MSCs can inhibit the expression of key enzymes involved in glucose metabolism (*GLUT1*, *HK2*, *PFK-1*, *LDHA*), as well as the JAK-STAT and PI3K-Akt signaling pathways in splenic CD4⁺ T lymphocytes of MRL/lpr mice. Janus kinases (JAKs) are intracellular protein tyrosine kinases, of these, and four of these have been identified in mammals: JAK1, JAK2, JAK3, and TYK2. JAK1, JAK2, and TYK2 are broadly expressed in various cell types, whereas JAK3 is expressed only in hematopoietic cells [50]. Seven mammalian STAT proteins (STAT1-4, STAT5A, STAT5B, and STAT6) are classic transcription factors that regulate gene transcription via DNA regulatory elements [51]. The JAK-STAT signaling pathway mediates more than 50 cytokines, growth factors, and hormones. O'Brien et al. showed that targeting the JAK-STAT signaling pathway by JAK inhibitors reduces the levels of glycolysis in synovial fibroblasts [52]. Feng et al. demonstrated that the glycolytic levels of glioma cells were inhibited by blocking the glucose transporter 4-mediated activation of JAK-STAT pathway [53]. Moreover, the JAK/STAT pathway regulates the expression of key glycolytic genes, including *Glut-1*, *PFK3B*, *PDK1*, *HK2*, and *GSK3A* [54]. Thus, the JAK-STAT pathway can directly or indirectly regulate and affect T cell metabolism. Direct regulation includes targeting STATs and controlling the expression of enzymes, transporters, and helper protein-coding genes associated with the metabolic pathways. Indirect regulation involves STATs-controlled expression of transcription factors, cytokine receptors, and other genes, which in turn, regulate the expression or function of components in the metabolic pathway [55]. The PI3K-Akt pathway is involved in various functions such as cell cycle, apoptosis, angiogenesis, and glucose metabolism. Akt is a downstream effector of PI3K activated by phosphorylation during transport from the cytoplasm to the cell membrane. The PI3K-Akt pathway is an upstream pathway of mTOR that regulates glucose metabolism levels through HIF-1 α [56]. The PI3K/AKT/mTOR pathway regulates many metabolic pathways, including glycolysis, OXPHOS, pentose phosphate, and tricarboxylic acid cycle [57]. Therefore, this and previous studies suggested that the mechanism by which hUC-MSCs regulate glucose metabolism in SLE-CD4⁺ T cells might be related to the JAK-STAT and PI3K-Akt pathways.

Our findings suggest that the *VEGFA*, *IL-10*, *HSP90AA1*, *IFNB1*, *F2R*, and *NR4A1* genes may contribute to the therapeutic mechanism of hUC-MSCs in SLE correlating to the

JAK-STAT and PI3K-Akt signaling pathways. Nevertheless, the exact interactions of these genes require further investigation through *in vivo* experiments. Of note, after co-culturing, the concentration of IL-10 in the supernatant of CD4⁺ T cells increased, while the mRNA expression of IL-10 decreased. This discrepancy may arise because mRNA levels do not always accurately reflect the corresponding protein levels. Cells may enhance IL-10 protein transport through post-translational modifications (e.g., phosphorylation and glycosylation) and post-transcriptional regulatory mechanisms, thereby increasing its secretion [58]. Furthermore, IL-10 is regulated by a negative feedback mechanism that allows cells to modulate its gene expression [59].

As an emerging treatment for SLE, hUC-MSCs have been confirmed to be effective and safe in clinical trials; However, the specific regulatory mechanisms remain unclear. This study showed pronounced abnormalities in the glucose metabolism levels of peripheral blood SLE-CD4⁺ T cells and explored the effects and possible mechanisms of hUC-MSCs on glucose metabolism in CD4⁺ T cells *in vitro*. There are some limitations in this study, such as the small sample size of SLE patients, only the protein levels of some key genes in the signaling pathway were verified, and the *in vitro* functional verification experiments of the activation or inhibition of the signaling pathway were not performed. We intend to further expand the sample size based on this study, including the inclusion of SLE patients with different levels of disease activity and lupus model mice with different stages of disease, in order to further clarify the therapeutic effects, long-term efficacy, and molecular regulatory mechanisms based on glucose metabolism of MSCs.

Conclusion

hUC-MSCs effectively inhibited the proliferation and function of the aberrant CD4⁺ T cells in patients with SLE, by regulating cellular glycometabolism and the JAK-STAT and PI3K-Akt signaling pathways, indicating a new insight into the therapeutic mechanism of MSCs based on metabolic reprogramming.

Abbreviations

SLE	Systemic lupus erythematosus
MSCs	Mesenchymal stem cells
hUC-MSCs	Human umbilical cord-derived mesenchymal stem cells
BMI	Body mass index
SLEDAI-2K	Systemic Lupus Erythematosus Disease Activity Index 2000
CCK	Cell proliferation detection by cell counting kit

OCR	Oxygen consumption rate
ECAR	Extracellular acidification rate
glycoPER	Glycolytic proton efflux rate
DEGs	Differentially expressed genes
q-PCR	Real-time quantitative polymerase chain reaction
HE	Hematoxylin eosin
WB	Western blot
CBB	Coomassie brilliant blue
PBS	Phosphate buffered saline
SRC	Spare respiratory capacity
OXPPOS	Oxidative phosphorylation
IFN- γ	Interferon-gamma
IL	Interleukin
TNF- α	Tumor necrosis factor-alpha
KEGG	Kyoto Encyclopedia of Genes and Genomes
GO	Gene Ontology
PPI	Protein-protein interaction network
GLUT1	Glucose transporter type 1
HK2	Hexokinase 2
PFK-1	Phosphofructokinase-1
LDHA	Lactate dehydrogenase A
STAT	Signaling transducers and transcriptional activator
mTOR	Mammalian target of rapamycin
HIF-1 α	Hypoxia-inducible factor-1 α
JAKs	Janus kinases
PTKs	Protein tyrosine kinases

Acknowledgements We thank Prof. Shaohua Wang, Department of Clinical Laboratory, The Second Hospital of Hebei Medical University for technical help in cell co-culture.

Author Contributions LAJ and MJ designed the study protocol. DM, JL, CSX, YL and WQ collected and analyzed clinical data of the patients. HJJ, WXP, CF, LX and YJJ conducted lab data analysis. SSR performed auto-antibody detection. DM, JL, CSX and YL drafted the manuscript. LAJ, MJ, SM and JHT revised the manuscript critically for important intellectual content. All authors approved the final version of the article. All had access to all study data and take responsibility for data integrity and accuracy. The corresponding author attests that all listed authors meet authorship criteria and that no others meeting the criteria have been omitted.

Funding This work was supported by the grants from Natural Science Foundation of Hebei Province (H2019206387, H2023206264), S&T Program of Hebei (19277721D), Clinical Medicine Excellent Talent Project of Hebei Government Foundation(303-2021-58-181, ZF2025100), Medical Science Research Project of Hebei (20240127) and Cultivation Program of National Nature Science Foundation of China (2HN202514).

Data Availability The datasets supporting the conclusions of this article are included within the article. Further information can be obtained from the corresponding author on reasonable request.

Declarations

Ethics Approval and Consent to Participate The study was approved by the Ethics Committee of the Second Hospital of Hebei Medical University (2021-R392) and the Animal Experimentation Committee of Hebei Medical University (2023-AE-164). All participants provided written informed consent.

Consent for Publication Not applicable.

Competing Interests The authors declare that they have no competing interests.

Open Access This article is licensed under a Creative Commons Attribution-NonCommercial-NoDerivatives 4.0 International License, which permits any non-commercial use, sharing, distribution and reproduction in any medium or format, as long as you give appropriate credit to the original author(s) and the source, provide a link to the Creative Commons licence, and indicate if you modified the licensed material. You do not have permission under this licence to share adapted material derived from this article or parts of it. The images or other third party material in this article are included in the article's Creative Commons licence, unless indicated otherwise in a credit line to the material. If material is not included in the article's Creative Commons licence and your intended use is not permitted by statutory regulation or exceeds the permitted use, you will need to obtain permission directly from the copyright holder. To view a copy of this licence, visit <http://creativecommons.org/licenses/by-nc-nd/4.0/>.

References

1. Tsokos, G. C. (2024). The immunology of systemic lupus erythematosus. *Nature Immunology*, 25, 1332–43. <https://doi.org/10.1038/s41590-024-01898-7>
2. Tenbrock, K., Rauen, T. (2022). T cell dysregulation in SLE. *Clinical Immunology*, 239, 109031. <https://doi.org/10.1016/j.clim.2022.109031>
3. Tanaka, Y., Kubo, S., Iwata, S., Yoshikawa, M., Nakayama, S. (2018). B cell phenotypes, signaling and their roles in secretion of antibodies in systemic lupus erythematosus. *Clinical Immunology*, 186, 21–5. <https://doi.org/10.1016/j.clim.2017.07.010>
4. Perl, A. (2017). Review: Metabolic control of immune system activation in rheumatic diseases. *Arthritis and Rheumatism*, 69, 2259–70. <https://doi.org/10.1002/art.40223>
5. Sharabi, A., Tsokos, G. C. (2020). T cell metabolism: new insights in systemic lupus erythematosus pathogenesis and therapy. *Nature Reviews Rheumatology*, 16, 100–12. <https://doi.org/10.1038/s41584-019-0356-x>
6. Frauwirth, K. A., Riley, J. L., Harris, M. H., Parry, R. V., Rathmell, J. C., Plas, D. R., Elstrom, R. L., June, C. H., Thompson, C. B. (2002). The CD28 signaling pathway regulates glucose metabolism. *Immunity*, 16, 769–77. [https://doi.org/10.1016/s1074-7613\(02\)00323-0](https://doi.org/10.1016/s1074-7613(02)00323-0)
7. Vander, H. M., Cantley, L. C., Thompson, C. B. (2009). Understanding the Warburg effect: the metabolic requirements of cell proliferation. *Science*, 324, 1029–33. <https://doi.org/10.1126/science.1160809>
8. Yin, Y., Choi, S. C., Xu, Z., Perry, D. J., Seay, H., Croker, B. P., Sobel, E. S., Brusko, T. M., Morel, L. (2015). Normalization of CD4+T cell metabolism reverses lupus. *Science Translational Medicine*, 7, 274ra18. <https://doi.org/10.1126/scitranslmed.aaa0835>
9. Munoz-Urbano, M., Quintero-Gonzalez, D. C., Vasquez, G. (2022). T cell metabolism and possible therapeutic targets in systemic lupus erythematosus: a narrative review. *Immunopharmacology and Immunotoxicology*, 44, 457–70. <https://doi.org/10.1080/08923973.2022.2055568>
10. Kaul, A., Gordon, C., Crow, M. K., Touma, Z., Urowitz, M. B., van Vollenhoven, R., Ruiz-Irastorza, G., Hughes, G. (2016). Systemic lupus erythematosus. *Nature Reviews. Disease Primers*, 2, 16039. <https://doi.org/10.1038/nrdp.2016.39>
11. Fanouriakis, A., Kostopoulou, M., Alunno, A., Aringer, M., Bajema, I., Boletis, J. N., Cervera, R., Doria, A., Gordon, C., Govoni, M., Houssiau, F., Jayne, D., Kouloumas, M., Kuhn, A., Larsen, J. L., Lerstrom, K., Moroni, G., Mosca, M., Schneider, M.,... Boumpas, D. T. (2019). 2019 update of the EULAR recommendations for the management of systemic lupus erythematosus. *Annals of the Rheumatic Diseases*, 78, 736–45. <https://doi.org/10.1136/annrheumdis-2019-215089>
12. Chan, J., Walters, G. D., Puri, P., Jiang, S. H. (2023). Safety and efficacy of biological agents in the treatment of Systemic Lupus Erythematosus (SLE). *Bmc Rheumatology*, 7, 37. <https://doi.org/10.1186/s41927-023-00358-3>
13. Wang, D., Huang, S., Yuan, X., Liang, J., Xu, R., Yao, G., Feng, X., Sun, L. (2017). The regulation of the Treg/Th17 balance by mesenchymal stem cells in human systemic lupus erythematosus. *Cellular & Molecular Immunology*, 14, 423–31. <https://doi.org/10.1038/cmi.2015.89>
14. Luz-Crawford, P., Kurte, M., Bravo-Alegria, J., Contreras, R., Nova-Lamperti, E., Tejedor, G., Noel, D., Jorgensen, C., Figueroa, F., Djouad, F., Carrion, F. (2013). Mesenchymal stem cells generate a CD4+CD25+Foxp3+regulatory T cell population during the differentiation process of Th1 and Th17 cells. *Stem Cell Research & Therapy*, 4, 65. <https://doi.org/10.1186/scrt216>
15. Krampera, M., Glennie, S., Dyson, J., Scott, D., Laylor, R., Simpson, E., Dazzi, F. (2003). Bone marrow mesenchymal stem cells inhibit the response of naive and memory antigen-specific T cells to their cognate peptide. *Blood*, 101, 3722–9. <https://doi.org/10.1182/blood-2002-07-2104>
16. Luz-Crawford, P., Djouad, F., Toupet, K., Bony, C., Franquesa, M., Hoogduijn, M. J., Jorgensen, C., Noel, D. (2016). Mesenchymal stem cell-derived interleukin 1 receptor antagonist promotes macrophage polarization and inhibits B Cell differentiation. *Stem Cells*, 34, 483–92. <https://doi.org/10.1002/stem.2254>
17. Liu, Y., Yin, Z., Zhang, R., Yan, K., Chen, L., Chen, F., Huang, W., Lv, B., Sun, C., Jiang, X. (2014). MSCs inhibit bone marrow-derived DC maturation and function through the release of TSG-6. *Biochemical and Biophysical Research Communications*, 450, 1409–15. <https://doi.org/10.1016/j.bbrc.2014.07.001>
18. Spaggiari, G. M., Capobianco, A., Abdelrazik, H., Becchetti, F., Mingari, M. C., Moretta, L. (2008). Mesenchymal stem cells inhibit natural killer-cell proliferation, cytotoxicity, and cytokine production: role of indoleamine 2,3-dioxygenase and prostaglandin E2. *Blood*, 111, 1327–33. <https://doi.org/10.1182/blood-2007-02-074997>
19. Yang, Q., Liu, Y., Chen, G., Zhang, W., Tang, S., Zhou, T. (2021). An overview of the safety, efficiency, and signal pathways of stem cell therapy for systemic lupus erythematosus. *Stem Cells International*, 2021, 2168595. <https://doi.org/10.1155/2021/2168595>
20. Aringer, M., Costenbader, K., Daikh, D., Brinks, R., Mosca, M., Ramsey-Goldman, R., Smolen, J. S., Wofsy, D., Boumpas, D. T., Kamen, D. L., Jayne, D., Cervera, R., Costedoat-Chalumeau, N., Diamond, B., Gladman, D. D., Hahn, B., Hiepe, F., Jacobsen, S., Khanna, D.,... Johnson, S. R. (2019). 2019 European League Against Rheumatism/American College of Rheumatology classification criteria for systemic lupus erythematosus. *Annals of the*

- Rheumatic Diseases*, 78, 1151–9. <https://doi.org/10.1136/annrheumdis-2018-214819>
21. Dominici, M., Le Blanc, K., Mueller, I., Slaper-Cortenbach, I., Marini, F., Krause, D., Deans, R., Keating, A., Prockop, D., Horwitz, E. (2006). Minimal criteria for defining multipotent mesenchymal stromal cells. The International Society for Cellular Therapy position statement. *Cytotherapy*, 8, 315–7. <https://doi.org/10.1080/14653240600855905>
 22. Veldhoen, M., Blankenhans, B., Konjar, S., Ferreira, C. (2018). Metabolic wiring of murine T cell and intraepithelial lymphocyte maintenance and activation. *European Journal of Immunology*, 48, 1430–40. <https://doi.org/10.1002/eji.201646745>
 23. Titchenell, P. M., Lazar, M. A., Birnbaum, M. J. (2017). Unraveling the Regulation of Hepatic Metabolism by Insulin. *Trends in Endocrinology and Metabolism*, 28, 497–505. <https://doi.org/10.1016/j.tem.2017.03.003>
 24. Saadh, M. J., Kazemi, K., Khorramdelazad, H., Mousavi, M. J., Noroozi, N., Masoumi, M., Karami, J. (2023). Role of T cells in the pathogenesis of systemic lupus erythematosus: Focus on immunometabolism dysfunctions. *International Immunology*, 119, 110246. <https://doi.org/10.1016/j.intimp.2023.110246>
 25. van der Windt, G. J., O'Sullivan, D., Everts, B., Huang, S. C., Buck, M. D., Curtis, J. D., Chang, C. H., Smith, A. M., Ai, T., Faubert, B., Jones, R. G., Pearce, E. J., Pearce, E. L. (2013). CD8 memory T cells have a bioenergetic advantage that underlies their rapid recall ability. *Proceedings National Academy of Sciences. United States of America*, 110, 14336–41. <https://doi.org/10.1073/pnas.1221740110>
 26. Wang, R., Dillon, C. P., Shi, L. Z., Milasta, S., Carter, R., Finkelstein, D., McCormick, L. L., Fitzgerald, P., Chi, H., Munger, J., Green, D. R. (2011). The transcription factor Myc controls metabolic reprogramming upon T lymphocyte activation. *Immunity*, 35, 871–82. <https://doi.org/10.1016/j.immuni.2011.09.021>
 27. Yin, Y., Choi, S. C., Xu, Z., Zeumer, L., Kanda, N., Croker, B. P., Morel, L. (2016). Glucose oxidation is critical for CD4+T cell activation in a mouse model of systemic lupus erythematosus. *Journal of Immunology*, 196, 80–90. <https://doi.org/10.4049/jimmunol.1501537>
 28. Kempkes, R., Joosten, I., Koenen, H., He, X. (2019). Metabolic Pathways Involved in Regulatory T Cell Functionality. *Frontiers in Immunology*, 10, 2839. <https://doi.org/10.3389/fimmu.2019.02839>
 29. Shan, J., Jin, H., Xu, Y. (2020). T Cell Metabolism: A new perspective on Th17/Treg cell imbalance in systemic lupus erythematosus. *Frontiers in Immunology*, 11, 1027. <https://doi.org/10.3389/fimmu.2020.01027>
 30. Wilson, C. S., Stocks, B. T., Hoopes, E. M., Rhoads, J. P., McNew, K. L., Major, A. S., Moore, D. J. (2021). Metabolic preconditioning in CD4+T cells restores inducible immune tolerance in lupus-prone mice. *Jci Insight*, 6. <https://doi.org/10.1172/jci.insight.143245>
 31. Doherty, E., Oaks, Z., Perl, A. (2014). Increased mitochondrial electron transport chain activity at complex I is regulated by N-acetylcysteine in lymphocytes of patients with systemic lupus erythematosus. *Antioxidants & Redox Signaling*, 21, 56–65. <https://doi.org/10.1089/ars.2013.5702>
 32. Yennemadi, A. S., Keane, J., Leisching, G. (2023). Mitochondrial bioenergetic changes in systemic lupus erythematosus immune cell subsets: Contributions to pathogenesis and clinical applications. *Lupus*, 32, 603–11. <https://doi.org/10.1177/09612033231164635>
 33. Xu, Y., Chen, Y., Zhang, X., Ma, J., Liu, Y., Cui, L., Wang, F. (2022). Glycolysis in innate immune cells contributes to autoimmunity. *Frontiers in Immunology*, 13, 920029. <https://doi.org/10.3389/fimmu.2022.920029>
 34. Crisan, M., Yap, S., Casteilla, L., Chen, C. W., Corselli, M., Park, T. S., Andriolo, G., Sun, B., Zheng, B., Zhang, L., Norotte, C., Teng, P. N., Traas, J., Schugar, R., Deasy, B. M., Badyrak, S., Buhning, H. J., Giacobino, J. P., Lazzari, L., ... Peault, B. (2008). A perivascular origin for mesenchymal stem cells in multiple human organs. *Cell Stem Cell*, 3, 301–13. <https://doi.org/10.1016/j.stem.2008.07.003>
 35. Cao, W., Cao, K., Cao, J., Wang, Y., Shi, Y. (2015). Mesenchymal stem cells and adaptive immune responses. *Immunology Letters*, 168, 147–53. <https://doi.org/10.1016/j.imlet.2015.06.003>
 36. Liu, J., Lu, X., Lou, Y., Cai, Y., Cui, W., Wang, J., Nie, P., Chen, L., Li, B., Luo, P. (2019). Xenogeneic transplantation of human placenta-derived mesenchymal stem cells alleviates renal injury and reduces inflammation in a mouse model of lupus nephritis. *Biotechnology Research International*, 2019, 9370919. <https://doi.org/10.1155/2019/9370919>
 37. Barbado, J., Tabera, S., Sanchez, A., Garcia-Sancho, J. (2018). Therapeutic potential of allogeneic mesenchymal stromal cells transplantation for lupus nephritis. *Lupus*, 27, 2161–5. <https://doi.org/10.1177/0961203318804922>
 38. Glennie, S., Soeiro, I., Dyson, P. J., Lam, E. W., Dazzi, F. (2005). Bone marrow mesenchymal stem cells induce division arrest anergy of activated T cells. *Blood*, 105, 2821–7. <https://doi.org/10.1182/blood-2004-09-3696>
 39. Cheng, A., Choi, D., Lora, M., Shum-Tim, D., Rak, J., Colmegna, I. (2020). Human multipotent mesenchymal stromal cells cytokine priming promotes RAB27B-regulated secretion of small extracellular vesicles with immunomodulatory cargo. *Stem Cell Research & Therapy*, 11, 539. <https://doi.org/10.1186/s13287-020-02050-6>
 40. Jang, E., Jeong, M., Kim, S., Jang, K., Kang, B. K., Lee, D. Y., Bae, S. C., Kim, K. S., Youn, J. (2016). Infusion of Human Bone Marrow-Derived Mesenchymal Stem Cells Alleviates Autoimmune Nephritis in a Lupus Model by Suppressing Follicular Helper T-Cell Development. *Cell Transplantation*, 25, 1–15. <https://doi.org/10.3727/096368915X688173>
 41. Huang, S., Wu, S., Zhang, Z., Deng, W., Fan, J., Feng, R., Kong, W., Qi, J., Chen, W., Tang, X., Yao, G., Feng, X., Wang, D., Chen, H., Sun, L. (2018). Mesenchymal stem cells induced CD4+T cell apoptosis in treatment of lupus mice. *Biochemical and Biophysical Research Communications*, 507, 30–5. <https://doi.org/10.1016/j.bbrc.2018.10.133>
 42. Franco, D. C. F., Andrade-Oliveira, V., Candido, D. A. D., Borges, D. S. T., Naffah, D. S. B. C., Costa, C. M., Faquim-Mauro, E. L., Antonio, C. M., Ioshie, H. M., Pacheco-Silva, A., Aparecida, C. R., Torrecilhas, A. C., Olsen, S. C. N. (2020). Extracellular Vesicles isolated from Mesenchymal Stromal Cells Modulate CD4(+) T Lymphocytes Toward a Regulatory Profile. *Cells-Basel*, 9. <https://doi.org/10.3390/cells9041059>
 43. Akhter, W., Nakhle, J., Vaillant, L., Garcin, G., Le Saout, C., Simon, M., Crozet, C., Djouad, F., Jorgensen, C., Vignais, M. L., Hernandez, J. (2023). Transfer of mesenchymal stem cell mitochondria to CD4(+) T cells contributes to repress Th1 differentiation by downregulating T-bet expression. *Stem Cell Research & Therapy*, 14, 12. <https://doi.org/10.1186/s13287-022-03219-x>
 44. Bottcher, M., Hofmann, A. D., Bruns, H., Haibach, M., Loschinski, R., Saul, D., Mackensen, A., Le Blanc, K., Jitschin, R., Mougiakakos, D. (2016). Mesenchymal Stromal Cells Disrupt mTOR-Signaling and Aerobic Glycolysis During T-Cell Activation. *Stem Cells*, 34, 516–21. <https://doi.org/10.1002/stem.2234>
 45. Talaat, R. M., Mohamed, S. F., Bassyouni, I. H., Raouf, A. A. (2015). Th1/Th2/Th17/Treg cytokine imbalance in systemic lupus erythematosus (SLE) patients: Correlation with disease activity. *Cytokine*, 72, 146–53. <https://doi.org/10.1016/j.cyto.2014.12.027>

46. Radmanesh, F., Mahmoudi, M., Yazdanpanah, E., Keyvani, V., Kia, N., Nikpoor, A. R., Zafari, P., Esmacili, S. A. (2020). The immunomodulatory effects of mesenchymal stromal cell-based therapy in human and animal models of systemic lupus erythematosus. *Lubmb Life*, 72, 2366–81. <https://doi.org/10.1002/iub.2387>
47. Khan, A., Ali, A. K., Marr, B., Jo, D., Ahmadvand, S., Fong-McMaster, C., Almutairi, S. M., Wang, L., Sad, S., Harper, M. E., Lee, S. H. (2023). The TNFalpha/TNFR2 axis mediates natural killer cell proliferation by promoting aerobic glycolysis. *Cellular & Molecular Immunology*, 20, 1140–55. <https://doi.org/10.1038/s41423-023-01071-4>
48. Wei, S., Xie, S., Yang, Z., Peng, X., Gong, L., Zhao, K., Zeng, K., Lai, K. (2019). Allogeneic adipose-derived stem cells suppress mTORC1 pathway in a murine model of systemic lupus erythematosus. *Lupus*, 28, 199–209. <https://doi.org/10.1177/0961203318819131>
49. Reyhani, S., Abbaspanah, B., Mousavi, S. H. (2020). Umbilical cord-derived mesenchymal stem cells in neurodegenerative disorders: from literature to clinical practice. *Regenerative Medicine*, 15, 1561–78. <https://doi.org/10.2217/rme-2019-0119>
50. Hu, X., Li, J., Fu, M., Zhao, X., Wang, W. (2021). The JAK/STAT signaling pathway: from bench to clinic. *Signal Transduction and Targeted Therapy*, 6, 402. <https://doi.org/10.1038/s41392-021-00791-1>
51. Morris, R., Kershaw, N. J., Babon, J. J. (2018). The molecular details of cytokine signaling via the JAK/STAT pathway. *Protein Science*, 27, 1984–2009. <https://doi.org/10.1002/pro.3519>
52. O'Brien, A., Hanlon, M. M., Marzaioli, V., Wade, S. C., Flynn, K., Fearon, U., Veale, D. J. (2021). Targeting JAK-STAT signaling alters PsA synovial fibroblast pro-inflammatory and metabolic function. *Frontiers in Immunology*, 12, 672461. <https://doi.org/10.3389/fimmu.2021.672461>
53. Feng, Y., Wang, J., Cai, B., Bai, X., Zhu, Y. (2022). Ivermectin accelerates autophagic death of glioma cells by inhibiting glycolysis through blocking GLUT4 mediated JAK/STAT signaling pathway activation. *Environmental Toxicology*, 37, 754–64. <https://doi.org/10.1002/tox.23440>
54. McGarry, T., Orr, C., Wade, S., Biniecka, M., Wade, S., Gallagher, L., Low, C., Veale, D. J., Fearon U. (2018). JAK/STAT blockade alters synovial bioenergetics, mitochondrial function, and proinflammatory mediators in rheumatoid arthritis. *Arthritis & Rheumatology*, 70, 1959–70. <https://doi.org/10.1002/art.40569>
55. Villarino, A. V. (2023). Transcriptional programming of T cell metabolism by STAT family transcription factors. *European Journal of Immunology*, 53, e2048825. <https://doi.org/10.1002/eji.202048825>
56. Agani, F., Jiang, B. H. (2013). Oxygen-independent regulation of HIF-1: novel involvement of PI3K/AKT/mTOR pathway in cancer. *Current Cancer Drug Targets*, 13, 245–51. <https://doi.org/10.2174/1568009611313030003>
57. Lien, E. C., Lyssiotis, C. A., Cantley, L. C. (2016). Metabolic reprogramming by the PI3K-Akt-mTOR pathway in cancer. *Recent Results in Cancer Research*, 207, 39–72. https://doi.org/10.1007/978-3-319-42118-6_3
58. Rutz, S., Ouyang, W. (2016) Regulation of Interleukin-10 expression. *Advances in Experimental Medicine and Biology*, 941, 89–116. https://doi.org/10.1007/978-94-024-0921-5_5
59. Ridley, M. L., Fleskens, V., Roberts, C. A., Lalnunhlmi, S., Alnesf, A., O'Byrne, A. M., Steel, K., Povoleri, G., Sumner, J., Lavender, P., Taams, L. S. (2020). IKZF3/Aiolos is associated with but not sufficient for the expression of IL-10 by CD4(+) T cells. *Journal of Immunology*, 204, 2940–8. <https://doi.org/10.4049/jimmunol.1901283>

Publisher's Note Springer Nature remains neutral with regard to jurisdictional claims in published maps and institutional affiliations.